ATTEST

Ref. Ares(2020)7533471 - 11/12/2020

WP2

Toolbox specification, support tools and test cases

Day-ahead and real-time optimization tools to support MES aggregators

D2.5

This project has received funding from the European Union's Horizon 2020 research and innovation programme under grant agreement No 864298.

DOCUMENT CONTROL PAGE

DOCUMENT	D2.5 – Day-ahead and real-time optimization tools to support MES aggregators
TYPE	Other
DISTRIBUTION LEVEL	Public
DUE DELIVERY DATE	31 / 10 / 2020
DATE OF DELIVERY	11 / 12 / 2020
VERSION	V1.0
DELIVERABLE RESPONSIBLE	INESC TEC
AUTHOR(S)	António Coelho and Filipe Soares (INESC TEC)
OFFICIAL REVIEWER(S)	Tomislav Capuder (ICENT) and Kaan Hakan (Techrain)

DOCUMENT HISTORY

VERSION	AUTHORS	DATE	CHANGES
0.1	António Coelho INESC TEC	15 / 10 / 2020	Document creation
0.2	António Coelho, Filipe Soares INESC TEC	31 / 10 / 2020	First complete version
0.5	António Coelho INESC TEC	30 / 11 / 2020	Addressing reviewers' comments
1.0	André Madureira INESC TEC	11 / 12 / 2020	Final version

Table of Contents

List of Figures

List of Tables

Abbreviations and Acronyms

ACCRONYM / ABBREVIATION	Extensive form
AC	Alternating current
ADMM	Alternating direction method of multipliers
AGC	Automatic gain control
COP	Coefficient of performance
DA	Day-ahead
DH	District heating
DSO	Distribution system operator
HEMS	Home energy management system
MES	Multi-energy system
MIBEL	Iberian Electricity Market
MV	Medium voltage
OPF	Optimal power flow
PV	Photovoltaic
RT	Real-time
SOC	State-of-charge

Nomenclature

Indices and sets

$d \in \{E, G, H\}$	Energy vectors (E: energy, G: gas, H: heat)
$j \in J$	Clients
$J_n \subset J$	Clients per bus n
k	ADMM iteration
$m, n, i \in N^E, N^G, N^H$	Buses/nodes of electricity, gas, and heat networks
$(m, n), (\mathrm{j}, \mathrm{i}) \in B^E, B^G, B^H$	Lines/pipelines from bus m to bus n for electricity, gas, and heat networks
$v \in T$	Flexible resources
$t, y \in T$	Time intervals

Parameters

C	Capacity of thermal buildings (J/kg.°C)
C_p	Specific heat of water (kWh/°C)
D^{DA}	Electricity downward bid calculated by the DA tool (MWh)
K_2	Value of gas well
$\overline{\ell}$	Square of the maximum current magnitude (p.u.)
L	Length of pipeline (m)
$\overline{m}, \underline{m}$	Maximum, minimum district heating mass flow of pipelines (kg/s)
$\overline{m_q}, \underline{m_q}$	Maximum, minimum district heating mass flow of nodes (kg/s)
P^{AGC}	AGC power signal (MWh)
$\overline{P^{DH}}, \underline{P^{DH}}$	Maximum, minimum district heating load power (kW)
$\overline{P^{EH}}, \underline{P^{EH}}$	Maximum, minimum electric heater power (kW)
$\overline{P^{EH-DH}}, \underline{P^{EH-DH}}$	Maximum, minimum electric heater power connected to DH (kW)
$P^{E,DA}$	Electricity energy bid calculated by the DA tool (MWh)
$\overline{P^{GH}}, \underline{P^{GH}}$	Maximum, minimum gas heater power (kW)
$\overline{P^{GH-DH}}, \underline{P^{GH-DH}}$	Maximum, minimum gas heater power connected to DH (kW)
$\overline{p^g}, \underline{p^g}$	Maximum, minimum gas well pressure (Bar)
$\overline{P^g}, \underline{P^g}$	Maximum, minimum gas well production (MWh)
$P^{G,DA}$	Gas energy bid calculated by the DA tool (MWh)

$\overline{p^h}, \underline{p^h}$	Maximum, minimum district heating pressure (MWh)
P^{IL}	Inflexible energy consumption (kW)
$\overline{P^{sto}}$	Maximum charging, discharging power of the storage systems (kW)
Pr^{PV}	Forecasted PV generation (MW)
Q^I	Reactive power injection (p.u.)
r	Resistance (p.u.)
R	Resistance of thermal buildings (°C/kW)
S^b	Base power (kVA)
$\overline{SOC}, \underline{SOC}$	Maximum, minimum state-of-charge of storage systems (MWh)
T_a	Ambient temperature (°C)
T_o	Outlet node temperature of heat loads (°C)
T_s	Supply node temperature of heat generators (°C)
$\overline{T}, \underline{T}$	Maximum, minimum pipeline temperature (°C)
$\overline{T_s}, \underline{T_s}$	Maximum, minimum supply node temperature (°C)
$\overline{T_o}, \underline{T_o}$	Maximum, minimum outlet node temperature(°C)
U^{DA}	Electricity upward bid calculated by the DA tool (MWh)
$\bar{v}, \underline{v}$	Square of the maximum,minimum voltage magnitude (p.u.)
x	Reactance (p.u.)
Δt	Length of the time interval t (h)
λ	Heat transfer coefficient (W/°C)
λ^B	Electricity secondary reserve band price (€/MWh)
$\lambda^{B,-}$	Electricity secondary reserve imbalance band price (€/MWh)
λ^D	Electricity secondary reserve upward activation price (€/MWh)
λ^E	Energy electricity price (€/MWh)
$\lambda^{E,-}$	Electricity energy negative imbalance price (€/MWh)
$\lambda^{E,+}$	Electricity energy positive imbalance price (€/MWh)
λ^G	Gas energy prices (€/MWh)
$\lambda^{G,-}$	Gas energy negative imbalance prices (€/MWh)
$\lambda^{G,+}$	Gas energy positive imbalance prices (€/MWh)
λ^U	Electricity secondary reserve downward activation price (€/MWh)

θ^D	Downward secondary reserve ratio
θ^U	Upward secondary reserve ratio
θ^o	Outdoor temperature (℃)
$\bar{\theta}$	Maximum temperature of comfort (℃)
$\underline{\theta}$	Minimum temperature of comfort (℃)
ϑ	Heat gains and losses not modeled explicitly (℃)
β	Thermal constant
η^-,η^+	Discharging, charging efficiency of the storage systems
η	Efficiency/coefficient of performance of resources
ρ	Penalty of the augmented Lagrangian (€/kW^2)
π	Penalty of the augmented Lagrangian (€/kW^2)

Continuous variables

D^{DA}	Day-ahead downward band bid power (MW)
D^{DH}	Downward district heating band bid power (MW)
D^E	Downward electricity band bid power(MW)
D^{EH}	Downward band bid power of electrical heaters in buildings (MW)
D^{EH-DH}	Downward band bid power of electrical heaters connected to DH(MW)
D^{PV}	Downward band bid power of PV systems (MW)
D^{RT}	Real-time downward band bid power (MV)
D^{sto}	Downward band bid power of storage systems (MW)
ℓ	Square of the current magnitude (p.u.)
m	Mass flow of pipelines (kg/s)
$\mathrm{m_q}$	Mass flows of heat loads and generators (kg/s)
U^{DA}	Day-ahead upward band bid power (MW)
U^{DH}	Upward district heating band bid power (MW)
U^E	Upward electricity band bid power(MW)
U^{EH}	Upward band bid power of electrical heaters in buildings (MW)
U^{EH-DH}	Upward band bid power of electrical heaters connected to DH (MW)
U^{PV}	Upward band bid power of PV systems (MW)
U^{RT}	Real-time upward band bid power (MW)
U^{sto}	Upward band bid power of storage systems (MW)

p^g	Gas pressure (Bar)
p^h	Heat pressure (Pas)
P	Power (kW)
P^{CU}	Power curtailed from PV systems (kWh)
P^{DA}	Day-ahead energy bid power (MWh)
P^{DH}	Power from district heating (kWh)
P^E	Electric energy bid power (MWh)
P^{EH}	Power from electrical heaters connected to the buildings (kWh)
P^{EH-DH}	Power from electrical heaters connected to the DH (kWh)
$P^{E,RT}$	Real-time energy bid power (MWh)
P^F	Active power flow (p.u.)
P^g	Power of gas consumed/generated (kWh)
P^G	Gas energy bid power (MWh)
P^{GH}	Power from gas heaters connected to the buildings (kWh)
P^{GH-DH}	Power from gas heaters connected to the DH (kWh)
P^H	Heat energy bid power (MWh)
P^{IL}	Power consumed by inflexible loads (kWh)
P^{PV}	Power generated by PV sytems (kWh)
P^v	Activated power from flexible resources (kWh)
$\hat{P}, \hat{P}^E, \hat{P}^G, \hat{P}^H$	Duplicate variables of P, P^E, P^G, P^H (MWh)
P^+, P^-	Charging, discharging power of storage systems (kW)
Q^F	Reactive power flow (p.u.)
$\mathrm{q}^{\mathrm{in}}, q^{out}$	Gas flows (kWh)
SOC	State-of-charge (kWh)
T	Temperature of pipelines (℃)
$\mathrm{T_s}$	Temperature of supply nodes (℃)
T_o	Temperature of outlet nodes (℃)
v	Square of the voltage magnitude (p.u.)
ΔD	Downward band bid variation power (MW)
$\Delta P^{E,-}$	Real-time energy bid negative variation electrical power (MWh)
$\Delta P^{E,+}$	Real-time energy bid positive variation electrical power (MWh)

$\Delta P^{G,-}$	Real-time energy bid negative variation gas power (MWh)
$\Delta P^{G,+}$	Real-time energy bid positive variation gas power (MWh)
ΔU	Upward band bid variation power (MW)
φ	Auxiliary binary variable
θ	Temperature (℃)
π	Dual variables of the augmented Lagrangian (€/kW)

Executive Summary

This report follows deliverable D2.5 “Day-ahead and real-time optimization tools to support MES aggregators”, a software that consists of the day-ahead and real-time optimization tools to support MES aggregators, which has been developed within task T2.5 of the ATTEST project.

1. Introduction

This report presents the algorithms developed under the framework of task T2.5 "Day-ahead and real-time optimization tools to support multi-energy system (MES) aggregators". The optimization tools developed will support the participation of MES aggregators in energy and ancillary services markets. Optimization tools for day-ahead (DA) and real-time (RT) were developed. The day-ahead optimization tool defines bids for the electricity and gas energy markets and bids for electricity ancillary services markets. The real-time management algorithm dispatches the operation of the MES and ensures the reliable delivery of the energy and ancillary services traded by the aggregator in the day-ahead markets. Both day-ahead and real time approaches include steady state modelling of the electricity, district heating and gas networks so that day-ahead bids and actual realizations are technically feasible. This task will feed the electricity market simulation platform (described in task T2.6) with day-ahead and real-time market behaviours of MES aggregators.

2. Description of the tools

The tools presented in this document are optimization tools to support the participation of MES aggregators in energy and ancillary services day-ahead and real-time markets.

The aggregator participates in the electricity energy and secondary reserve markets and in the gas energy market. The tertiary markets usually have significantly lower activation ratios and thus, it was not considered in these tools.

The optimization tools are divided into day-ahead and real-time approaches. The day-ahead optimization tool defines bids for the energy and ancillary services markets. The real-time management algorithm dispatches the operation of the MES and ensures the reliable delivery of the energy and ancillary services traded by the aggregator in the day-ahead markets.

Both day-ahead and real time approaches include steady state modelling of the electricity, district heating and gas networks so that day-ahead bids and actual realizations are technically feasible. This task will feed the electricity market simulation platform (described in task T2.6) with day-ahead and real-time market behaviors of MES aggregators.

The aggregator has the purpose of minimizing costs in the participation in the energy markets while fulfilling the energy needs of its customers. It is thus able to exploit the flexibility offered by their resources including PV systems, storage systems and thermal loads, by controlling electric heaters installed in the buildings and in the district heating network.

The aggregator optimizes the market bids and then negotiates with the distribution system operator (DSO) of the electricity, gas and district heating networks in order to compute network-secure energy and secondary reserve bids from the distribution networks' perspective. When the negotiation is concluded, the final bids calculated by the aggregator are offered in the respective markets.

The real-time tool is a hierarchical model predictive control that dispatches the flexible resources and delivers the energy and secondary reserve considering the DA bids.

The aggregator acts as a price taker by submitting non-priced demand and supply bids to the day-ahead electricity and gas energy market. Aggregators communicate with his customers through home energy management system (HEMS) [1].

Thus, these tools are able to optimize the aggregator's bids considering its role within the day-ahead and real-time energy markets and the contracts with his clients while making them network-secure. A scheme of the operational model for the day-ahead and real-time tools are presented in Figure 1 and Figure 2 - Real-time tool scheme. It is possible to observe that the inputs necessary to run the model are energy prices from electricity and gas markets, technical constraints from buildings, power, gas and heat networks and weather forecasts. The outputs of the optimization are electricity and gas market bids per hour per bus. The inputs and outputs of these tools are described in detail in Chapter 0. A more detailed description of this model is presented in Chapters 0, 0 and 0.

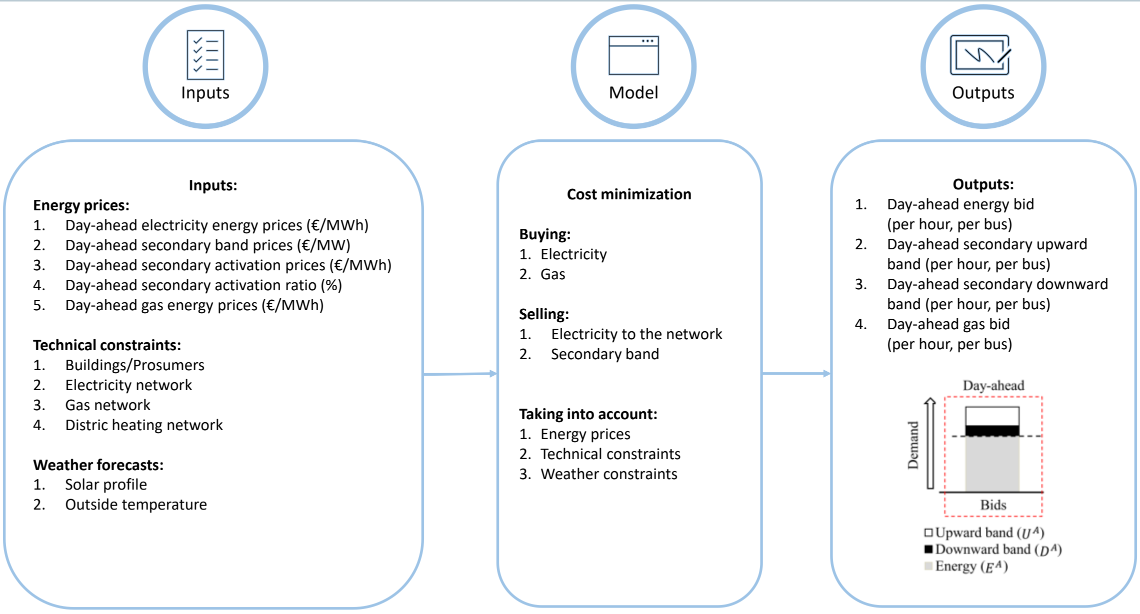

FIGURE 1 – DAY-AHEAD TOOL SCHEME

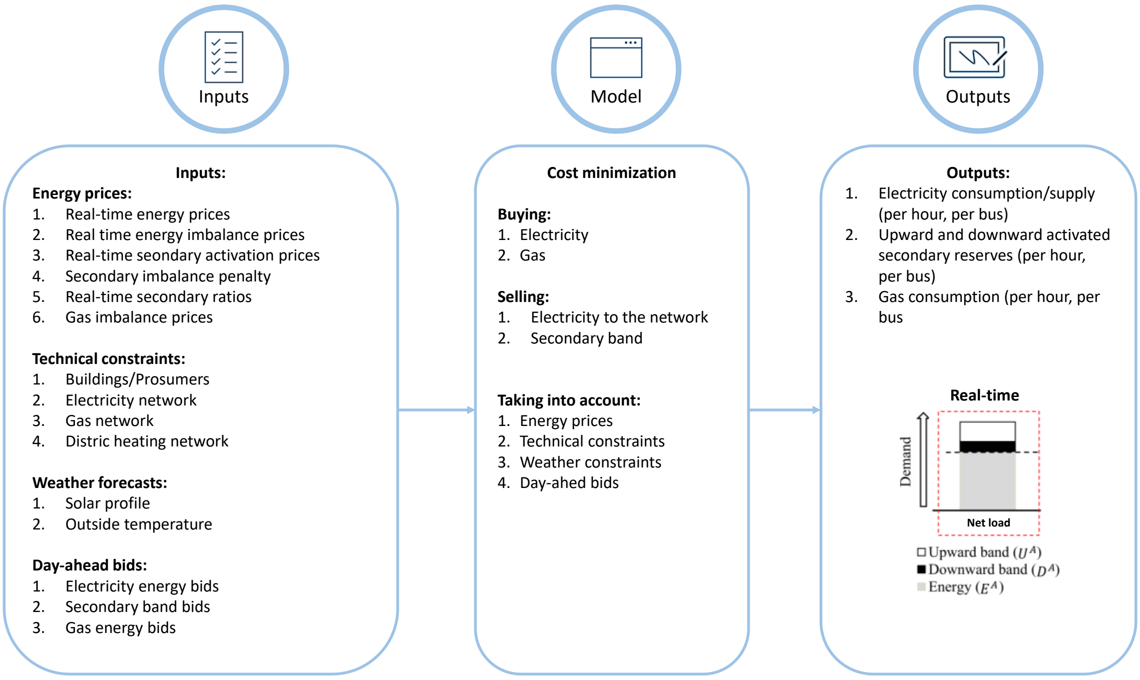

FIGURE 2 - REAL-TIME TOOL SCHEME

3. Inputs and outputs

In this chapter, the inputs necessary to run the tools developed and their outputs are presented. The input and outputs data format is in *Excel (xlsx)* format. Annex I includes the information about the *Excel* files with examples of input and output data.

3.1. Inputs

The inputs of the day-ahead and real-time tools are presented in the following tables. They incorporate the parameters of the buildings and consumers, electrical, gas and heat network parameters and also weather forecasts. In the case of the real-time tool the inputs of the accepted bids in the DA market are also necessary.

The parameters necessary to model the loads, buildings or resources are the constraints of the electrical heaters, gas heaters, PV systems, storage systems, district heating connection, gas load thermal model characteristics and energy consumption.

TABLE 1 – BUILDING PARAMTERS

Load/Building/Resource		
Electrical heater	Installed	0 - no, 1 - yes
	Maximum power	kW
	Efficiency/COP	-
Gas heater	Installed	0 - no, 1 - yes
	Maximum power	kW
	Efficiency/COP	-
PV	Installed	0 - no, 1 - yes
	Maximum power	kW
Storage	Installed	0 - no, 1 - yes
	Maximum power	kW
	Maximum SOC	kWh
	Mininum SOC	kWh
	Initial SOC	kWh
	Efficiency	-
District heating	Installed	0 - no, 1 - yes
	Maximum power	kW
Gas	Load	0 - no, 1 - yes
Thermal model building	Resistance	ºC /kW
	Capacity	kWh/ ºC
	Initial temperature	ºC
	Maximum and mininum temperature per hour	ºC
Energy consumption	Electricity consumption	kWh
	Gas consumption	kWh
	Heat consumption	kWh

The parameters of the electrical network are branch and buses parameters and the power system base.

TABLE 2 - ELECTRICAL NETWORK PARAMETERS

Electrical network		
	Parameter	**Unit**
Branches	Branch connections	-
	R	Ω
	X	Ω
	Branch limits	A
Buses	Voltage limits	p.u.
	Reference bus number	-
	Reference bus voltage	p.u.
	Load/building/resource connections	-
	System base	MVA

The parameters of the gas network are pipeline and buses parameters.

TABLE 3 - GAS NETWORK PARAMETERS

Gas network		
	Parameter	**Unit**
Pipeline	Pipeline connections	-
	Length	m
	Diameter	mm
Buses	Pressure limit	Bar
	Reference bus number	-
	Load/building/resource connections	-

The parameters of the heat network are related with the loads, generators, pipelines and buses. The extreme buses and middle buses location indicate the buses that are on the extremes of the network and have heat loads and the middle buses are the buses that are on the middle of the network and have heat loads.

TABLE 4 - HEAT NETWORK PARAMETERS

Heat network		
	Parameter	Unit
Load	Location	-
	Return temperature	ºC
Generator	Type	w – electricity g - gas
	Electrical, gas and heat bus connection	-
	Supply node temperature	ºC
	Power limits	kW
	Efficiency/COP	-
Pipeline	Connections	-
	Length	m
	Diameter	mm
	Heat transfer coefficient	W/ºC
	Supply pipeline temperature limits	ºC
	Return pipeline temperature limits	ºC
	Pipeline mass flow limits	kg/s
	Ambient temperature	ºC
	Friction of pipeline	-
Buses	Supply bus temperature limits	ºC
	Return bus temperature limits	ºC
	Pressure limits	Pa
	Load/building/resource connections	-

The weather inputs are the forecasted solar profile and outside temperature.

TABLE 5 - WEATHER PARAMETERS

Weather	
Parameter	Unit
Solar profile	%
Outside temperature	ºC

The input prices for the day-ahead tool are the electricity and gas day-ahead markets and electricity secondary reserve markets. It is also necessary the forecasted activation ratios of the secondary reserves.

TABLE 6 - PRICES FOR DAY-AHEAD TOOL

Prices – Day-ahead tool		
	Parameter	Unit
Electricity	Day-ahead energy prices	€/MWh
	Secondary reserve day-ahead energy prices – upward and downward	€/MWh
	Secondary reserve ratios – upward and downward	%
Gas	Day-ahead energy prices	€/MWh

The inputs prices for the real-time tool are the real-time energy prices, energy imbalance prices, secondary reserve activation prices, secondary reserve imbalance penalties, secondary reserve activation ratios and gas imbalance prices.

TABLE 7 - PRICES FOR REAL-TIME TOOL

Prices – Real-time tool		
	Parameter	**Unit**
Electricity	Real-time energy prices	€/MWh
	Real-time energy imbalances prices – positive and negative	€/MWh
	Real-time secondary reserve activation prices – upward and downward	€/MWh
	Secondary reserve imbalance penalty	€/MWh
	Real-time secondary reserve ratios – upward and downward	%
Gas	Gas imbalance prices – positive and negative	€/MWh

For the real-time tool it is necessary to have the day-ahead electricity energy and secondary reserve band bids as well as the gas energy bids offered in the markets as inputs. It is also necessary to have the automatic gain control (AGC) signal.

TABLE 8 - DAY-AHEAD BIDS FOR REAL-TIME TOOL

Day-ahead bids – Real-time tool		
	Parameter	**Unit**
Electricity	Day-ahead energy bids	MWh
	Day-ahead secondary reserve band bids – upward and downward	MW
Gas	Day-ahead energy bids	MWh
AGC	AGC signal	MWh

3.2. Outputs

The outputs of the day-ahead tool are the electricity and gas market bids per hour per bus.

TABLE 9 - OUTPUTS OF THE DAY-AHEAD TOOL

Energy bids – Day-ahead tool		
	Parameter	**Unit**
Electricity	Energy bid (per hour, per electrical bus)	MWh
	Upward secondary reserve band bid (per hour, per electrical bus)	MW
	Downward secondary reserve band bid (per hour, per electrical bus)	MW
Gas	Energy bid (per hour, per gas node)	MWh

The outputs of the real-time tool are the electricity energy consumption/supply, activated secondary reserves and gas energy consumption.

TABLE 10 - OUTPUTS OF THE REAL-TIME TOOL

Energy consumption – Real-time tool		
	Parameter	**Unit**
Electricity	Energy consumption/supply (per hour, per electrical bus)	MWh
	Activated secondary upward reserve (per hour, per electrical bus)	MW
	Activated secondary downward reserve (per hour, per electrical bus)	MW
Gas	Energy consumption (per hour, per node bus)	MWh

4. Methodology

4.1. General description

The tools developed in this work have the objective of minimizing aggregator's costs in participating in day-ahead and real-time energy markets while taking into account network constraints.

In order to optimize aggregator's bids and consider energy network constraints, a decentralized approach based on the alternating direction method of multipliers (ADMM) was developed (Figure 3). The aggregators negotiate with the DSOs of each of the energy networks and obtain solutions that satisfy the consumption scenarios and network constraints. This approach takes the optimization problem into sub-problems and solves each one of them separately and iteratively until it reaches convergence. The final bids calculated by the ADMM in the day-ahead tool are submitted to the day-ahead markets and the final net load and reserves activated are dispatched in real-time. Section 4.2 provides more details of the strategy ADMM approach.

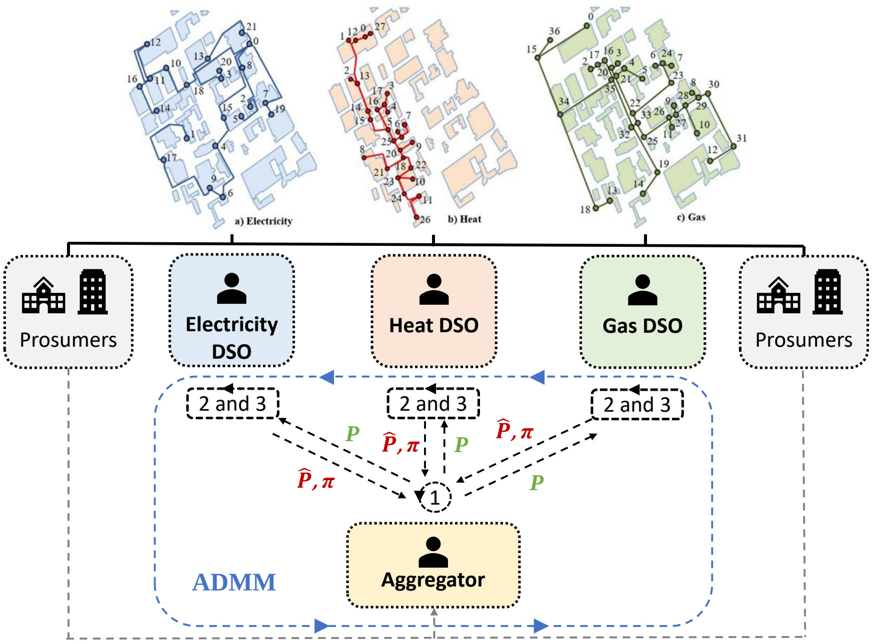

FIGURE 3 - ADMM ALGORITHM

In the day-ahead tool, the aggregator runs its algorithm for 24h in order to calculate the day-ahead bids and negotiates with each energy DSOs, following the ADMM approach. Each DSO runs the respective energy flow for each hour of the day. Then, they continue negotiating energy delivery scenarios until convergence is reached. The final bids calculated by the aggregator are submitted to the day-ahead markets.

In the real-time tool, the aggregator has two levels: a deterministic optimization level and a controller level (Figure 4). In the deterministic optimization level, the aggregator runs its algorithm for the next hour in order to define the operating points and upward and downward secondary reserve bands of the aggregator. Following the ADMM approach, it negotiates with the respective energy DSOs in order to make the energy scenarios feasible until convergence is reached. Then, the controller of the second level adjusts the operating points considering the ones calculated at level 1 for that hour and the AGC signal, which is run each 10 seconds.

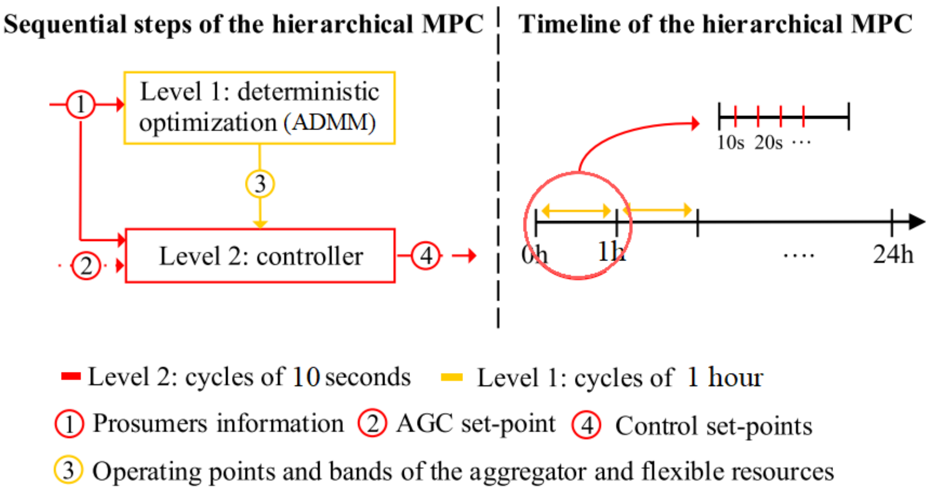

FIGURE 4 - AGGREGATOR REAL-TIME HIERARCHICAL CONTROL [2]

Prosumer's in this tool can be modelled with the following characteristics:

- Connection with the electrical, gas and heat networks;
- Electrical, gas and heat inflexible loads;
- Thermal loads;
- Electrical or gas heaters (boilers, heat pumps, etc);
- Storage systems;
- PV systems

The aggregator optimizes these resources while satisfying the prosumers' energy needs. The interactions are made through a HEMS. The electrical heaters connected to buildings with thermal loads or to the district heating are sources of demand flexibility, storage systems are sources of demand and generation flexibility and PV systems are sources of generation flexibility. A source of demand flexibility means that the resource is able to decrease or increase consumption and a source of generation flexibility means that the resource is able to decrease or increase generation. The prosumers with thermal loads modeled have to define their temperature range setpoints for each hour. The optimization constraints of the aggregator and prosumers for the day-ahead and real-time are detailed in Chapter 0.

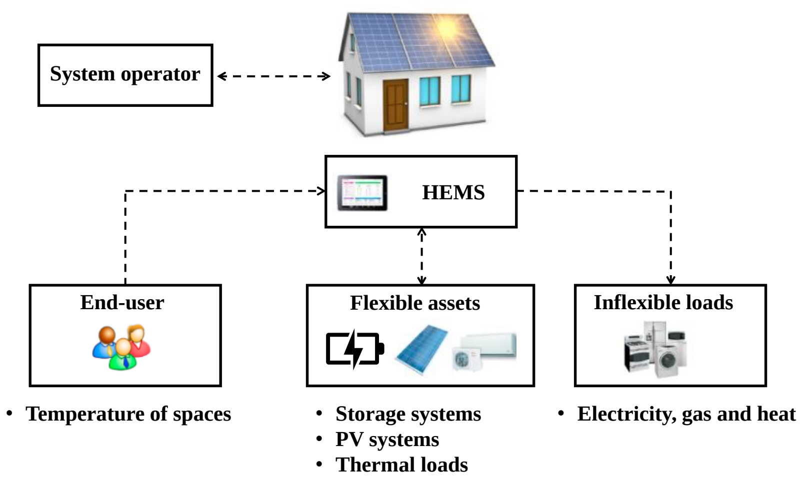

FIGURE 5 - FLOW OF INFORMATION BETWEEN AGGREGATOR AND PROSUMERS (ADAPTED FROM [1])

In order to evaluate their network feasibility, the electricity DSO runs an alternating-current optimal power flow (AC OPF), the gas DSO runs a non-linear steady-state gas flow and the heat DSO runs a non-linear heat flow, including hydraulic and thermal modelling of the network. The constraints of electrical, gas and heat flow are presented in Chapter 0.

The energy scenarios represent the energy consumption in the respective period when reserves are not activated, the upward scenarios represent the energy consumption when upward reserves are activated and downward scenarios represent energy consumption when downward reserves are activated. The electricity DSO runs downward and upward scenarios, the gas DSO runs an energy scenario and the heat DSO runs an energy, downward and upward scenarios.

The tools were implemented in Python 3.7 and this is a requirement to run them. The aggregator problem is solved by mixed-integer linear programming algorithm of the *IBM CPLEX v12.9.0* optimizer, which requires a license, and the electricity, gas and heat flows are solved by non-linear programming algorithm of the *IPOPT v3.11.1 optimizer*.

4.2. Network-constrained bidding optimization strategy

This section describes the optimization strategy developed in this work.

The optimization problem can be represented by (1)-(13). The objective function of the aggregator is represented by $f_a$and its internal inputs by X_a. The energy exchange scenarios between the aggregator and the operators of each energy network are represented by P_a. The constraint functions of the aggregator is represented by (2). The constraints function of the DSOs are represented by (3) and Y represents their internal inputs. Variables $\widehat{P}$ are duplicates of the variable P, so that each aggregator have the energy exchanged into account. Constraint (4) enforces the same value of the duplicate variables to enable the decomposition of the optimization problem [3].

$$min \sum_{a \in A} f_a(P_a, X_a) \tag{1}$$

$$h_a(P_a, X_a) \leq 0, \qquad \forall \; a \in A \tag{2}$$

$$g(\hat{P}, Y) \leq 0 \tag{3}$$

$$P - \hat{P} = 0 \tag{4}$$

The ADMM algorithm is used to decompose the optimization problem into aggregator and electrical, gas and heat DSOs problems. The bidding problem of the aggregator is presented in (5) and (6).

$$P^{(k+1)} = \; min \; f_a(P_a, X_a) + \sum_{d \in \{E,G,H\}} \mathcal{L}_a^d(P_a, \hat{P}_a^{\;(k)}, \pi_a^{(k)}) \tag{5}$$

$$h_a(P_a, X_a) \leq 0 \tag{6}$$

The optimization problem of each energy DSO is represented in (7) and (8).

$$\hat{P}^{d,(k+1)} = \min \mathcal{L}^d(P^{d,(k+1)}, \hat{P}^d, \pi^{d,k}) \tag{7}$$

$$g(\hat{P}^d, Y^d) \leq 0 \tag{8}$$

$\mathcal{L}$ is the penalty term of the augmented Lagrangian applied to the equality constraint (9), where π is a vector with dual variables and ρ is the penalty of the augmented Lagrangian.

$$\mathcal{L}(P, \hat{P}, \pi) = \pi^{\mathrm{T}}(P - \hat{P}) + \frac{\rho}{2}\|P - \hat{P}\|_2^2 \tag{9}$$

The dual variables pi are updated following equation (10).

$$\pi^{(k+1)} = \pi^{(k)} + \rho(P^{(k+1)} - \hat{P}^{(k+1)}) \quad (10)$$

The penalty term ρ can be modified at each iteration to accelerate the convergence of the algorithm. The update in the day-ahead tool is described in equation (11). Auxiliary variable $count$ starts at 0 and is incremented by 1 each time the algorithm does not satisfy the restrictions $k > 0 \wedge R^D < 0.05 \wedge count \geq 5$.

$$\rho^{k+1} = \begin{cases} 0.05, if\ k = 0 \\ 2.\rho^k, if\ k > 0 \wedge R^D < 0.05 \wedge count \geq 5 \\ \rho^k, otherwise \end{cases} \quad (11)$$

The update in the real-time tool is described in equation (12). Auxiliary variable $count$ starts at 0 and is incremented by 1 each time the algorithm does not satisfy the restrictions $k > 0 \wedge count \geq 5$.

$$\rho^{k+1} = \begin{cases} 0.01, if\ k = 0 \\ \rho^k + 0.1, if\ k > 0 \wedge count \geq 5 \\ \rho^k, otherwise \end{cases} \quad (12)$$

The primal and dual criteria are calculated by (13) and (14), where the primal residual represents the violation of constraint (4) and the dual residual represents the violation of the Karush-Kuhn-Tucker stationarity constraint. The convergence is reached when the scaled 2-norm of both residuals are smaller than 0.05.

$$R^{P,(k+1)} = \left((P_1^{k+1} - \hat{P}_1^{k+1}), (P_2^{k+1} - \hat{P}_2^{k+1}), \dots\right)^T \quad (13)$$

$$R^{D,(k+1)} = \left(\rho(\hat{P}_1^{k+1} - P_1^k), \rho(\hat{P}_2^{k+1} - P_2^{k+1}), \dots\right)^T \quad (14)$$

The ADMM algorithm, as illustrated in Figure 3, is the following:

TABLE 11 - ADMM ALGORITHM

Algorithm 1: ADMM algorithm
1. Aggregator optimizes his bids by holding $\boldsymbol{\hat{P}^k}, \boldsymbol{\pi^k}$ constant at $\boldsymbol{k^{th}}$ values. Values of $\boldsymbol{P}$ are obtained;
2. DSOs solve their problem by holding $\boldsymbol{P^{d,k+1}}$, $\boldsymbol{\pi^{d,k}}$ constant and obtain the values of $\boldsymbol{\hat{P}^d}$.
2.1. Electrical DSO runs AC OPF for upward and downward scenarios;
2.2. Gas DSO runs non-linear steady state gas flow for upward and downward scenarios;
2.3. Heat DSO runs non-linear heat flow for energy, upward and downward scenarios;
3. Calculate primal residual $\boldsymbol{R^P}$ and dual residual $\boldsymbol{R^D}$ through (13) and (14):
3.1. If $\boldsymbol{R^P}, \boldsymbol{R^D}$< 0.05:
3.1.1. Save bids and stop algorithm;
3.2. Else:
3.2.1. Update $\boldsymbol{\pi}$ through (10);
3.2.2. Calculate new $\boldsymbol{\rho}$ through (12) or (13);
3.2.3. Back to step 1.

5. Aggregator optimization problem

In this chapter, the constraints of the aggregator problem are presented. The model for the day-ahead and real-time tool only differ in the objective function and certain market constraints which are presented below. The day-ahead bidding constraints, the bid delivery constraints and thermal, PV and storage systems constraints are the same for both tools.

5.1. Objective function and market constraints

5.1.1. Day-ahead

The objective of the optimization problem is to minimize the net cost of the aggregator of trading electricity in the energy and secondary reserve market and buying gas in the gas market as in equation (15) and (16). In (16), the first term is the net cost of buying or selling energy in the day-ahead market, the second term is the revenue of selling band in the reserve market and the third term is the revenue of mobilizing band in the secondary reserve market [1].

$$min \sum_{t \in T} \left[f_t + \sum_{d \in \{E,G,H\}} \sum_{n \in N^d} \mathcal{L}_{n,t}^d \right] \tag{15}$$

$$f_t = (\lambda_t^E P_t^{DA} + \lambda_t^G P_t^G)\Delta t - \lambda_t^B (U_t^{DA} + D_t^{DA}) + (\lambda_t^D \theta_t^D D_t^{DA} - \lambda_t^U \theta_t^U U_t^{DA})\Delta t \tag{16}$$

Constraint (17) defines that the secondary reserve band must be 2/3 for the upward band and 1/3 for the downward band, according to a rule from the Iberian Electricity Market (MIBEL) [1].

$$U_t^{DA} = 2.D_t^{DA}, \forall\, t \in T \tag{17}$$

$$P_t^{DA} = P_t^E, \forall\, t \in T \tag{18}$$

$$D_t^{DA} = D_t^E, \forall\, t \in T \tag{19}$$

$$U_t^{DA} = U_t^E, \forall\, t \in T \tag{20}$$

Equation (21) defines the penalty term of the augmented Lagrangian. It penalizes deviations from the networks optimization flows.

$$\mathcal{L}_{n,t}^d = {\pi_{n,t}^d}^{(k)} \left(P_{n,t}^d - \hat{P}_{n,t}^d\right) + \frac{\rho}{2}\left(P_{n,t}^d - \hat{P}_{n,t}^d\right)^2 \tag{21}$$

The energy and band bids have the duration of 1h Δt.

5.1.2. Real-time

5.1.2.1. Level 1: Deterministic optimization model

The objective of the optimization problem is to minimize the net cost of the aggregator of dispatching electricity traded in the day-ahead market and gas in the gas energy market, as in equation (22) and (23). In (23), the first term is the net cost of buying or selling energy in the RT market, the second term is the imbalance costs between DA electricity market commitments and RT deliveries, the third term is the costs of mobilizing downward and upward reserves, the fourth term is the penalty for band not supplied and the fifth term is the imbalance costs between DA gas market commitments and RT gas delivery [2].

$$min \sum_{t \in T} \left[f_t + \sum_{d \in \{E,G,H\}} \sum_{n \in N^d} \mathcal{L}_{n,t}^d \right] \tag{22}$$

$$f_t = \hat{\lambda}_t^E P_t^{E,RT} + \left(\hat{\lambda}_t^{E,-} \Delta P_t^{E,-} - \hat{\lambda}_t^{E,+} \Delta P_t^{E,+}\right) + \left(\hat{\lambda}_t^D \hat{\theta}_t^D D_t^{RT} - \hat{\lambda}_t^U \hat{\theta}_t^U U_t^{RT}\right)\Delta t + \lambda_t^{B,-}(\Delta U_t + \Delta D_t)\Delta \mathrm{t} + \left(\hat{\lambda}_t^{G,-} \Delta P_t^{G,-} - \hat{\lambda}_t^{G,+} \Delta P_t^{G,+}\right) \tag{23}$$

The imbalances between DA and RT electricity energy bids are presented in constraint (24). If energy imbalances are present, the aggregator cannot provide reserves, as seen in constraints (25) and (26), where φ_t is an auxiliary binary variable and M a big number. Constraints (27) and (28) define the upward and downward bands not supplied. Constraint (29) defines that the secondary reserve band must be 2/3 for the upward band and 1/3 for the downward band. Contraint (30) defines the gas imbalances in relation to the DA bids. Constraint (31) defines that $D_t^{RT}, U_t^{RT}, \Delta \mathrm{D_t}, \Delta U_\mathrm{t}, \Delta P_t^{E,-}$ and $\Delta P_t^{E,+}$ are positive. P_t^{RT} is negative for generation and positive for net consumption. It is important to note that in the real-time tool, P_t^{DA}, U_t^{DA} and D_t^{DA} are inputs of the model.

$$\Delta P_t^{E,-} - \Delta P_t^{E,+} = P_t^{E,RT} - P_t^{E,DA}, \forall\, t \in T \tag{24}$$

$$\Delta P_t^{E,-} + \Delta P_t^{E,+} \leq (1 - \varphi_t)M, \forall\, t \in T \tag{25}$$

$$D_t^{RT} + U_t^{RT} \leq \varphi_t(D^{DA} + U^{DA}), \forall\, t \in T \tag{26}$$

$$\Delta \mathrm{D_t} = D_t^{DA} - D_t^{RT}, \forall\, t \in T \tag{27}$$

$$\Delta \mathrm{U_t} = U_t^{DA} - U_t^{RT}, \forall\, t \in T \tag{28}$$

$$U_t^{RT} = 2. D_t^{RT}, \forall\, t \in T \tag{29}$$

$$\Delta P_t^{G,-} - \Delta P_t^{G,+} = P_t^{G,RT} - P_t^{G,DA}, \forall\, t \in T \tag{30}$$

$$D_t^{RT}, U_t^{RT}, \Delta \mathrm{D_t}, \Delta U_\mathrm{t}, \Delta P_t^{E,-}, \Delta P_t^{E,+} \geq 0, \forall\, t \in T \tag{31}$$

$$P_t^{E,RT} = P_t^E, \forall\, t \in T \tag{32}$$

$$D_t^{RT} = D_t^E, \forall\, t \in T \tag{33}$$

$$U_t^{RT} = U_t^E, \forall\, t \in T \tag{34}$$

$$P_t^{G,RT} = P_t^G, \forall\, t \in T \tag{35}$$

Equation (31) defines the penalty term of the augmented Lagrangian. It penalizes deviations from the networks' optimization flows.

$$\mathcal{L}_{n,t}^d = \pi_{n,t}^{d\ (k)}\left(P_{n,t}^d - \hat{P}_{n,t}^d\right) + \frac{\rho}{2}\left(P_{n,t}^d - \hat{P}_{n,t}^d\right)^2 \tag{36}$$

The energy and band bids have the duration of 1h Δt.

5.1.2.2. Level 2: Controller

The controller of the aggregator tracks the AGC signal and adjusts the operating points of the resources. The objective is to make the operating point of the aggregator equal to the AGC signal [2].

The new operating point is presented in constraints (37). The parameters $U_{i,t}^{v}/U_{t}^{RT}$ and $D_{i,t}^{v}/D_{t}^{RT}$ define the contribution of each resource to the AGC signal. ψ_h represents the power of the AGC, considering the operating points defined at level 1 and it is present in equation (38).

$$P_{i,h}^{v} = \begin{cases} P_{i,t}^{v} + \min(\psi_h(U_{i,t}^{v}/U_{t}^{RT}), U_{i,t}^{v}), \psi_h > 0 \land P_h^{AGC} \geq P_t^{RT} \\ P_{i,t}^{v} - \min(\psi_h(D_{i,t}^{v}/D_{t}^{RT}), D_{i,t}^{v}), \psi_h > 0 \land P_h^{AGC} < P_t^{RT}, \\ P_{i,t}^{v}, \psi_h = 0 \end{cases} \tag{37}$$
$$\forall\, v \in \{PV, EH, EH-DH, sto\}, i \in I^{v}$$

$$\psi_h = \begin{cases} \min(P_h^{AGC} - P_t^{RT}, U_t^{RT}), U^{RT} + D^{RT} > 0 \land P_h^{AGC} \geq P_t^{RT} \\ \min(P_t^{RT} - P_h^{AGC}, D_t^{RT}), U^{RT} + D^{RT} > 0 \land P_h^{AGC} < P_t^{RT} \\ 0, U_t^{RT} + D_t^{RT} = 0 \end{cases} \tag{38}$$

5.2. Bidding constraints

Constraints (39)-(42) define the electrical and gas energy, upward and downward day-ahead bids or real-time commitments of the aggregator. U_t^{E} and D_t^{E} take into account the reserves from storage systems, PV systems, electrical heaters connected to the buildings and electrical heaters connected to the district heating [3].

$$P_t^{E} = \sum_{n \in N^{E}} P_{n,t}^{E}, \quad \forall\, t \in T \tag{39}$$
$$P_t^{G} = \sum_{n \in N^{G}} P_{n,t}^{G}, \quad \forall\, t \in T \tag{40}$$
$$U_t^{E} = \sum_{j \in J_n} \left(U_{j,t}^{sto} + U_{j,t}^{PV} + U_{j,t}^{EH} + U_{j,t}^{EH-DH}\right), \quad \forall\, n \in N^{E}, t \in T \tag{41}$$
$$D_t^{E} = \sum_{j \in J_n} \left(D_{j,t}^{sto} + D_{j,t}^{PV} + D_{j,t}^{EH} + D_{j,t}^{EH-DH}\right), \quad \forall\, n \in N^{E}, t \in T \tag{42}$$

5.3. Delivery scenarios constraints

Delivery scenarios define possible exchanges of power between aggregators' clients and energy networks. The scenarios exchanged are for the upward $P_{n,t}^{U-E}$ and downward $P_{n,t}^{D-E}$ electricity scenarios, gas energy scenarios $P_{n,t}^{G}$ and energy $P_{n,t}^{H}$, upward $P_{n,t}^{U-H}$ and downward $P_{n,t}^{D-H}$ heat scenarios [3].

The electrical bid $P_{n,t}^{E}$ (43) results from the sum of the energy consumed by the inflexible electrical load, the electrical heaters directly connected to the buildings, the electrical heaters of the district heating and the electrical storage system; and the energy generated by the electrical storage system and the PV system.

$$P_{n,t}^{E} = \sum_{j \in J_n} (P_{j,t}^{IL-E} + P_{j,t}^{EH} - P_{jt}^{PV} + P_{j,t}^{+} - P_{j,t}^{-} + P_{j,t}^{EH-DH}), \; t \in T \tag{43}$$

The gas bid $P_{n,t}^{G}$ (44) results from the sum of the energy consumed by the gas loads of the buildings, the gas heaters connected to the buildings and the gas heaters connected to the district heating.

$$P_{n,t}^{G} = \sum_{j \in J_n} (P_{j,t}^{IL-G} + P_{j,t}^{GH} + P_{j,t}^{GH-DH}), \forall\, n \;\; t \in T \tag{44}$$

The heat bid $P_{n,t}^{H}$ (45) results from the sum of the energy consumed by the inflexible heating load, the heating power consumed by the buildings connected to the district heating and the energy generated by the electrical or gas heaters connected to the district heating.

$$P_{n,t}^{H} = \sum_{j\in J_n}(P_{j,t}^{IL-H} + P_{j,t}^{DH} - P_{j,t}^{EH-DH}.\eta_j^{EH} - P_{j,t}^{GH-DH}.\eta_j^{GH}), \forall\ t \in T \quad (45)$$

The upward band $P_{n,t}^{U-E}$ (46) defines the flexibility of electric heaters connected to the buildings, electric heaters connected to the district heating and storage system to decrease load and storage system and PV systems to increase generation.

$$P_{n,t}^{U-E} = P_{n,t}^{E} - \sum_{j\in J_n}\left(U_{j,t}^{sto} + U_{j,t}^{PV} + U_{j,t}^{EH} + U_{j,t}^{EH-DH}\right),\ \ \forall\, n \in N^{E}, t \in T \quad (46)$$

The downward band $P_{n,t}^{D-E}$ (47) defines the flexibility of electric heaters connected to the buildings, electric heaters connected to the district heating and storage systems to increase load and storage systems and PV systems to decrease generation.

$$P_{n,t}^{D-E} = P_{n,t}^{E} + \sum_{j\in J_n}\left(D_{j,t}^{sto} + D_{j,t}^{PV} + D_{j,t}^{EH} + D_{j,t}^{EH-DH}\right),\ \ \forall\, n \in N^{E}, t \in T \quad (47)$$

The upward band $P_{n,t}^{U-H}$ (48) defines the flexibility of the heating loads and electric heaters connected to the district heating to decrease load.

$$P_{n,t}^{U-H} = P_{n,t}^{H} - \sum_{j\in J_n}\left(U_{j,t}^{DH} + U_{j,t}^{EH-DH}.\eta_j^{EH}\right),\ \ \forall\, n \in N^{H}, t \in T \quad (48)$$

The downward band $P_{n,t}^{D-H}$ (49) defines the flexibility of the heating loads and electric heaters connected to the district heating to increase load.

$$P_{n,t}^{D-H} = P_{n,t}^{H} - \sum_{j\in J_n}\left(D_{j,t}^{DH} + D_{j,t}^{EH-DH}.\eta_j^{EH}\right),\ \ \forall n \in N^{H}, t \in T \quad (49)$$

5.4. Thermal system constraints

5.4.1. Building heaters

The electrical or gas heaters directly connected to the buildings are defined by equations (50)-(62). Equation (50) and (51) define the minimum and maximum limits of the electric and gas heaters. The electric or gas heater consumption of buildings with inflexible heating load is defined by equation (52); buildings with flexible load are defined by equations (53)-(62). Equations (53)-(58) define the thermal models of the buildings with electric or gas heaters. Equation (59)-(61) define the downward and upward bands of the electric heaters. Equation (62) defines the value of β [4].

$$\underline{P_{j,t}^{EH}} \le P_{j,t}^{EH} \le \overline{P_{j,t}^{EH}},\ \ \forall\ j \in J,\ \ t \in T \quad (50)$$

$$\underline{P_{j,t}^{GH}} \le P_{j,t}^{GH} \le \overline{P_{j,t}^{GH}},\ \ \forall\ j \in J,\ \ t \in T \quad (51)$$

$$P_{j,t}^{EH}.\eta^{EH} + P_{j,t}^{GH}.\eta^{GH} = P_{j,t}^{IL-H},\ \ \forall\ j \in J^{inf},\ \ t \in T \quad (52)$$

$$\theta_{j,t+1}^{E} = \beta_j\theta_{j,t}^{E} + (1-\beta_j)\left[\theta_{j,t}^{o} + R_j\left(\eta_j^{EH}P_{j,t}^{EH} + \eta_j^{GH}P_{j,t}^{GH}\right)\right] + \vartheta_{n,j,t},\ \forall\ j \in J,\ \ t \in T \quad (53)$$

$$\underline{\theta}_j \le \theta_{j,t+1}^{E} \le \overline{\theta}_j,\quad \forall\ j \in J,\ \ t \in O_j \quad (54)$$

$$\theta_{j,t+1}^{U} = \beta_j\theta_{j,t}^{U} + (1-\beta_j)\left[\theta_{j,t}^{o} + R_j\eta_j^{EH}\left(P_{j,t}^{EH} - U_{j,t}^{EH}\right)\right] + \vartheta_{n,j,t},\ \forall\ j \in J,\ \ t \in T \quad (55)$$

$$\underline{\theta}_j \le \theta_{j,t+1}^{U} \le \overline{\theta}_j,\quad \forall\ j \in J,\ \ t \in O_j \quad (56)$$

$$\theta_{j,t+1}^{D} = \beta_j\theta_{j,t}^{D} + (1-\beta_j)\left[\theta_{j,t}^{o} + R_j\eta_j^{EH}\left(P_{j,t}^{EH} + D_{j,t}^{EH}\right)\right] + \vartheta_{n,j,t},\ \forall\ j \in J,\ \ t \in T \quad (57)$$

$$\underline{\theta_j} \leq \theta_{j,t+1}^{D} \leq \overline{\theta}_j, \quad \forall\ j \in J,\ \ t \in O_j \tag{58}$$

$$D_{j,t}^{EH} \leq \overline{P_{j,t}^{EH}} - P_{j,t}^{EH}, \ \forall\ j \in J,\ \ t \in T \tag{59}$$

$$U_{j,t}^{EH} \leq \ P_{j,t}^{EH} - \underline{P_{j,t}^{EH}}, \ \forall\ j \in J,\ \ t \in T \tag{60}$$

$$D_{j,t}^{EH}, U_{j,t}^{EH} \geq 0, \ \ \forall\ j \in J,\ \ t \in T \tag{61}$$

$$\beta_j = e^{-\frac{1}{R_j \cdot C_j}}, \forall\ j \in J \tag{62}$$

5.4.2. District heating

The power consumed by the buildings connected to the district heating are defined by equation (63)-(71). Equation (63) defines the minimum and maximum limits of the power consumed by load from the district heating. The load consumption of the buildings with inflexible heating load is defined by equation (64); buildings with flexible load are defined by equations (65)-(71). Equations (65)-(68) define the thermal models of the buildings connected with the district heating. Equation (69)-(71) define the downward and upward bands.

$$\underline{P_{j,t}^{DH}} \leq P_{j,t}^{DH} \leq \overline{P_{j,t}^{DH}}, \ \forall\ j \in J,\ \ t \in T \tag{63}$$

$$P_{j,t}^{DH} = P_{j,t}^{IL-H}, \ \forall\ j \in J^{inf},\ \ t \in T \tag{64}$$

$$\theta_{j,t+1}^{U} = \beta_j \theta_{j,t}^{U} + (1-\beta_j)\left[\theta_{j,t}^{o} + R_j\left(P_{j,t}^{DH} - U_{j,t}^{DH}\right)\right] + \vartheta_{n,j,t}, \ \forall\ j \in J,\ \ t \in T \tag{65}$$

$$\underline{\theta_j} \leq \theta_{j,t+1}^{U} \leq \overline{\theta}_j, \quad \forall\ j \in J,\ \ t \in O_j \tag{66}$$

$$\theta_{j,t+1}^{D} = \beta_j \theta_{j,t}^{D} + (1-\beta_j)\left[\theta_{j,t}^{o} + R_j\left(P_{j,t}^{DH} + D_{j,t}^{DH}\right)\right] + \vartheta_{n,j,t}, \ \forall\ j \in J,\ \ t \in T \tag{67}$$

$$\underline{\theta_j} \leq \theta_{j,t+1}^{D} \leq \overline{\theta}_j, \quad \forall\ j \in J,\ \ t \in O_j \tag{68}$$

$$D_{j,t}^{DH} \leq \overline{P_{j,t}^{DH}} - P_{j,t}^{DH}, \ \forall\ j \in J,\ \ t \in T \tag{69}$$

$$U_{j,t}^{DH} \leq \ P_{j,t}^{DH} - \underline{P_{j,t}^{DH}}, \ \forall\ j \in J,\ \ t \in T \tag{70}$$

$$D_{j,t}^{DH}, U_{j,t}^{DH} \geq 0, \ \ \forall\ j \in J,\ \ t \in T \tag{71}$$

5.4.3. PV system constraints

Equation (72) defines the power generated by a PV. $Pr_{j,t}^{PV}$ is the forecasted PV generation. Equation (73) defines the curtailment limits of the PV system. Equation (74) and (75) define the upward and downward band limits [1].

$$P_{j,t}^{PV} = \ Pr_{j,t}^{PV} - P_{j,t}^{CU}, \ \forall\ \ j \in J,\ \ t \in T \tag{72}$$

$$0 \leq P_{j,t}^{CU} \leq Pr_{j,t}^{PV}, \ \forall\ \ j \in J,\ \ t \in T \tag{73}$$

$$0 \leq U_{j,t}^{PV} \leq P_{j,t}^{CU} \ \ \forall\ \ j \in J,\ \ t \in T \tag{74}$$

$$0 \leq D_{j,t}^{PV} \leq Pr_{j,t}^{PV} - P_{j,t}^{CU}, \ \forall\ \ j \in J,\ \ t \in T \tag{75}$$

5.4.4. Storage system constraints

The operation of storage units installed is defined by constraints (76)-(84). Equation (76) defines the SOC of the storage system. Equation (77) represents the storage limit capacity. Equations (78) and (79) set the range for charging and discharging power. Equation (80) sets the SOC of the battery for the first hour.

$$SOC_{j,t+1} = SOC_{j,t} + \left(P_{j,t}^{+}\eta_j^{+} - \frac{P_{j,t}^{-}}{\eta_j^{-}}\right)\Delta t, \ \forall\ \ j \in J,\ \ t \in T \tag{76}$$

$$\underline{SOC_j} \leq SOC_{j,t+1} \leq \overline{SOC_j}, \ \forall \ j \in J, \ t \in T \quad (77)$$

$$0 \leq P_{j,t}^{-} \leq \overline{P_j^{sto}}, \ \forall \ j \in J, \ t \in T \quad (78)$$

$$0 \leq P_{j,t}^{+} \leq \overline{P_j^{sto}}, \ \forall \ j \in J, \ t \in T \quad (79)$$

$$SOC_{j,-1} = SOC_j^{E}, \ \forall \ j \in J \quad (80)$$

The upward and downward bands provided by the batteries are defined by equations (81)-(84). Constraints (81) and (82) limit the downward $D_{j,t}^{sto}$ and upward $U_{j,t}^{sto}$ bands to the available charging and discharging powers, respectively. Constraints (83) and (84) guarantee that the EV only supply upward and downward bands if the SOC is within the minimum and maximum SOC_j.

$$0 \leq D_{j,t}^{sto} \leq \overline{P_j^{sto}} - P_{j,t}^{+}, \ \forall \ j \in J, \ t \in T_{j,t}^{sto} \quad (81)$$

$$0 \leq U_{j,t}^{sto} \leq \overline{P_j^{sto}} - P_{j,t}^{-}, \ \forall \ j \in J, \ t \in T_{j,t}^{sto} \quad (82)$$

$$U_{j,t}^{sto}, D_{j,t}^{sto} \leq \frac{\overline{SOC_j} - SOC_{j,t+1}}{\eta_j \Delta t}, \ \forall \ j \in J, \ t \in T_{j,t}^{sto} \quad (83)$$

$$U_{j,t}^{sto}, D_{j,t}^{sto} \leq \frac{(SOC_{j,t+1} - \underline{SOC_j})\eta_j}{\Delta t}, \ \forall \ j \in J, \ t \in T_{j,t}^{sto} \quad (84)$$

5.4.5. Electric and gas heaters

Equation (85) and (86) define the limits of the electric and gas heaters connected to the district heating. Equations (87)-(89) define the downward and upward band limits of the electric heaters.

$$\underline{P_{j,t}^{EH-DH}} \leq P_{j,t}^{EH-DH} \leq \overline{P_{j,t}^{EH-DH}}, \ \forall \ j \in J, \ t \in T \quad (85)$$

$$\underline{P_{j,t}^{GH-DH}} \leq P_{j,t}^{GH-DH} \leq \overline{P_{j,t}^{GH-DH}}, \ \forall \ j \in J, \ t \in T \quad (86)$$

$$D_{j,t}^{EH-DH} \leq \overline{P_{j,t}^{EH-DH}} - P_{j,t}^{EH-DH}, \ \forall \ j \in J, \ t \in T \quad (87)$$

$$U_{j,t}^{EH-DH} \leq P_{j,t}^{EH-DH} - \underline{P_{j,t}^{EH-DH}}, \ \forall \ j \in J, \ t \in T \quad (88)$$

$$D_{j,t}^{EH-DH}, U_{j,t}^{EH-DH} \geq 0, \ \forall \ j \in J, \ t \in T \quad (89)$$

6. Energy networks subproblems

6.1. Electricity network

6.1.1. Time horizon

The optimisation problem is decomposed by time-step $t \in T$. In the next subsections, we drop the subscripts of time $t \in T$ to increase readability.

6.1.2. Objective function

The optimisation model minimizes the augmented Lagrangian penalty (90). In this case, P is a parameter and $\hat{P}$ is a free variable.

$$min \sum_{n \in N^E} \left[\pi_n^E \left(P_n^E - \hat{P}_n^E\right) + \frac{\rho}{2}\left(P_n^E - \hat{P}_n^E\right)^2\right] \tag{90}$$

6.1.3. MV network constraints

The AC OPF is modelled using the branch flow formulation in the non-convex form and is defined by equations (91)-(94) [5].

$$P_{m,n}^F = \frac{\hat{P}_n^E}{S^B} + \sum_{i:n \to i} P_{n,i}^F + r_{m,n}\ell_{m,n}, \ (m,n) \in L^E \tag{91}$$

$$Q_{m,n}^F = Q_n^I + \sum_{i:n \to i} Q_{n,i}^F + x_{m,n}\ell_{m,n}, \ (m,n) \in L^E \tag{92}$$

$$v_n = v_m - 2\left(r_{m,n}P_{m,n}^F + x_{m,n}Q_{m,n}^F\right) + \left(r_{m,n}^2 + x_{m,n}^2\right)\ell_{m,n}, \ (m,n) \in L^E \tag{93}$$

$$\ell_{m,n}v_m = {P_{s,t,m,n}^F}^2 + {Q_{s,t,m,n}^F}^2, \ \forall\, (m,n) \in L^E \tag{94}$$

Equation (95) and (96) set the voltage and current magnitude limits.

$$\underline{v_n} \leq v_n \leq \overline{v_n}, \ \forall\, n \in N^E \tag{95}$$

$$0 \leq \ell_{m,n} \leq \overline{\ell_{m,n}}, \ \forall\, (m,n) \in L^E \tag{96}$$

6.2. Gas network

6.2.1. Time horizon

The optimisation problem is decomposed by time-step $t \in T$. In the next subsections, we drop the subscripts of time $t \in T$ to increase readability.

6.2.2. Objective function

The optimisation model minimizes the augmented Lagrangian penalty (97). In this case, P is a parameter and $\hat{P}$ is a free variable.

$$min \sum_{n \in N^G} \left[\pi_n^G \left(P_n^G - \hat{P}_n^G\right) + \frac{\rho}{2}\left(P_n^G - \hat{P}_n^G\right)^2\right] \tag{97}$$

6.2.3. Network constraints

Equation (98) and (99) limit the gas production and the nodal pressure.

$$\underline{P}_i^g \leq P_i^g \leq \overline{P}_i^g, \forall\, i \in N^G \tag{98}$$

$$\underline{p}_i^g \leq p_i^g \leq \overline{p}_i^g, \forall\, i \in N^G \tag{99}$$

The gas balance of each node is presented in the equation (100) and it takes into account the gas generation and consumption and the gas that goes in and out from the pipes connected to that node [6].

$$P_m^g - \hat{P}_n^G + \sum_{n \in m} q_{mn}^{out} - \sum_{n \in m} q_{mn}^{in} = 0, \forall\, m, n \in N^G, (m,n) \in B^G \tag{100}$$

For the steady-state case, the mass flow is assumed as constant in space. This means that the gas flowing into the pipe is equal to the gas flowing out of the pipe. Equation (101) defines the general steady-state general gas flow equation and can be determined by the incremental pressure between two end nodes of the pipeline [6].

$$sgn(\breve{q}_{mn})\breve{q}^2{}_{mn} = K_2(p_n^2 - p_m^2), \forall\, m, n \in N^G, (m,n) \in B^G \tag{101}$$

6.3. Heat network

6.3.1. Time horizon

The optimisation problem is decomposed by time-step $t \in T$. In the next subsections, we drop the subscripts of time $t \in T$ to increase readability.

6.3.2. Objective function

The optimisation model minimizes the augmented Lagrangian penalty (102). In this case, P is a parameter and $\hat{P}$ is a free variable.

$$min \sum_{n \in N^H} \left[\pi_n^H (P_n^H - \hat{P}_n^H) + \frac{\rho}{2}(P_n^H - \hat{P}_n^H)^2\right] \tag{102}$$

6.3.3. Network constraints

A heating network consists of supply and return networks. Both networks are coupled together as the mass flow rate in one pipe in the supply network is the same as the corresponding return pipe.

Hydraulic and thermal optimizations are carried out to determine the mass flows and temperatures of pipes and nodes [7].

6.3.3.1. Hydraulic model

The continuity of flow is expressed as: the mass flow that enters into a node is equal to the mass flow that leaves the node plus the flow consumption at the node. Equation (103) and (104) define the conservation of mass and pressure drop equations, assuming incompressible and constant water properties throughout the network. A is the network incidence matrix that relates nodes to branches. Equations (105)-(107) define the pressure and mass flow limits of pipelines and loads/generators [7].

$$A.\dot{m} = \dot{m}_q \tag{103}$$

$$p_j^h - p_i^h = K_{i,j}.\dot{m}_{j,i}.\left|\dot{m}_{j,i}\right|, \forall\, i, j \in N^H, (i,j) \in B^H, \tag{104}$$

$$\underline{p_j^h} \leq p_j^h \leq \overline{p_j^h}, \forall\, j\ \in N^H \quad (105)$$
$$\underline{m_{j,i}} \leq m_{j,i} \leq \overline{m_{j,i}}, \forall\, (j,i)\ \in B^H \quad (106)$$
$$\underline{m_{q,j,}} \leq m_{q,i} \leq \overline{m_{q,i}}, \forall\, i\ \in N^H \quad (107)$$

6.3.3.2. Thermal model

The thermal model is used to determine the temperatures at each supply and return node. There are three different temperatures associated with each node: the supply temperature T_s; the outlet temperature T_o and the return temperature T_r. The outlet temperature is defined as the temperature of the flow at the outlet of each node before mixing in the return network. If there is no flow mixing at a node, then the outlet temperature T_o is equal to the return temperature T_r at this node.

The equations which relate mass flow rate and temperature are the heat power equation, the temperature drop equations and conservation of energy.

The heat power consumed by loads and produced by generators are defined by equation (108) and (109).

$$\mathrm{P}_{n,i}^{IL-DH} = C_p.\dot{m}_{q,i}.\left(T_{s,i} - T_{o,i}\right), \forall\, i\ \in N^H \quad (108)$$
$$\hat{P}_{n,i}^{H} = -C_p.\dot{m}_{q,i}.\left(T_{s,i} - T_{o,i}\right), \forall\, i\ \in N^H \quad (109)$$

The temperature drop equation, which relates the two ends of the pipe, is derived from the heat loss equation and it is defined in equation (110). With the hot water circulating through the pipes, part of the heat is lost to the surrounding which causes the water temperature to drop along the pipe.

$$T_{i,j,out} = (T_{i,j,in} - T_a).e^{\frac{\lambda L}{C_p.\dot{m}_{i,j}}} + T_a, \qquad ,\forall\, (i,j)\ \in B^H \quad (110)$$

The conservation of energy relates the outgoing mass flow rates and water temperature at a given node j with all incoming mass flow rates and water temperatures (111). The temperature limits of pipelines and supply/outlet nodes are defined by equations (112)-(114).

$$\sum_j \left(T_{j,in}.\dot{m}_{j,in}\right) = T_{j,out}.\sum_j \left(\dot{m}_{j,out}\right), \forall\, j\ \in N^H \quad (111)$$
$$\underline{T_{i,j}} \leq T_{i,j} \leq \overline{T_{i,j}}, \forall\, (i,j)\ \in B^H \quad (112)$$
$$\underline{T_{s,j,}} \leq T_{s,i} \leq \overline{T_{s,i}}, \forall\, i\ \in N^H \quad (113)$$
$$\underline{T_{o,j,}} \leq T_{o,i} \leq \overline{T_{o,i}}, \forall\, i\ \in N^H \quad (114)$$

6.3.4. Direction flow

In order to calculate the direction of the mass flows, algorithm 2 is applied in the first iteration of the heat DSO negotiation where one heat flow is run with the loads calculated by the aggregator. In order to minimize the heat losses, the overall temperature of the network should be controlled as low as possible [8]. This way, the direction of the flow is calculated with the objective of minimizing heat losses.

TABLE 12 - HEAT DIRECTION FLOW

Algorithm 2: Heat direction flow
1. Set heat loads according to the aggregator optimization;
2. Set all the temperatures of pipelines, generators and loads to the lower limits;
3. Optimize production of heat sources and calculate mass flows;
4. Save direction of mass flows.

7. Results

In this chapter, the study case used to test the tools and the results obtained are presented.

7.1. Study case

The University of Manchester microgrid was used as the study case to test the tools [9]. It has electrical, heat and gas networks optimized by the tools. A scheme of the networks is presented in Figure 6. The electricity network has 22 buses in which 39 buildings are connected to them; bus 0 is the reference bus and it has two heat-pumps connected to bus 6 and 12. The heat network has 28 buses in which 21 buildings are connected to them and has two heat pumps connected to bus 0 and 26. The gas network has 36 buses in which 28 buildings are connected to them and bus 0 is the reference bus.

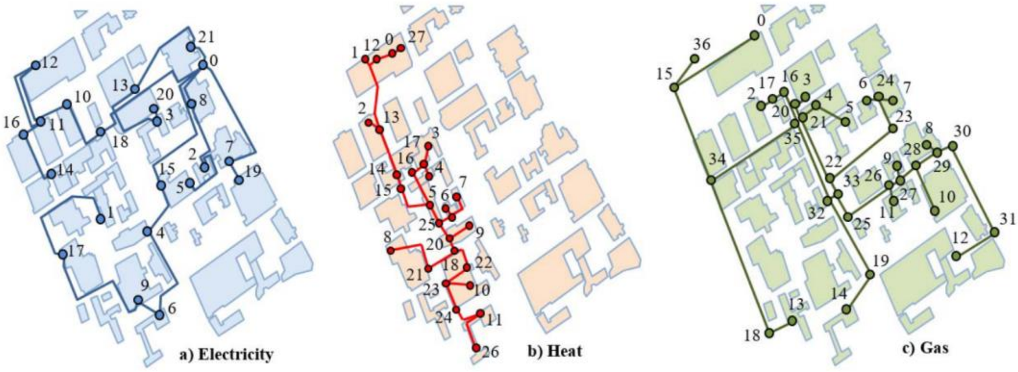

FIGURE 6 - ELECTRICAL, HEAT AND GAS NETWORKS OF THE STUDY CASE

All buildings have inflexible electrical and gas loads. Buildings 8, 11, 22, 34 and 39 are modelled as thermal models and have 0.75 MW heat pumps connected to the electrical network installed. Buildings 2, 13, 15, 25 and 32 are also modelled as thermal buildings but they are connected to the district heating network. They were modelled as large buildings, according to [10] and their resistance *R* was set to 0.081 ^{o}C/kWh and their capacity was set to 437.7 kWh/^{o}C. Heat pumps have a COP of 3.45.

Buildings 4, 8, 11, 12, 14, 24, 31, 33 and 34 have PV and storage systems installed. The total PV power installed is 2075 kW and the total capacity of storage systems is 418.5 kWh. The storage systems have an efficiency of 90% and their power has a range of 10 to 50 kW.

The power capacity of the two heat pumps that provide heat to the district heating was set to 10 MW each.

All the electricity prices were taken from [11][12] and the gas prices were taken from [13].

The electricity prices for the day-ahead tool are presented in Figure 7 and the secondary reserve activation ratios in Figure 8. The price of gas was set to 22.99 €/MWh.

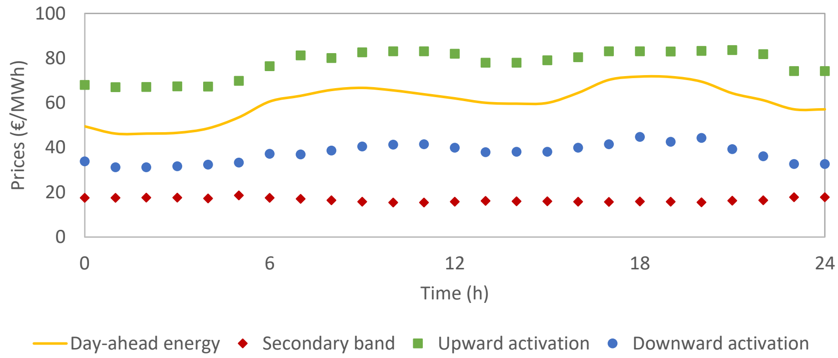

FIGURE 7 - DAY-AHEAD ELECTRICITY PRICES

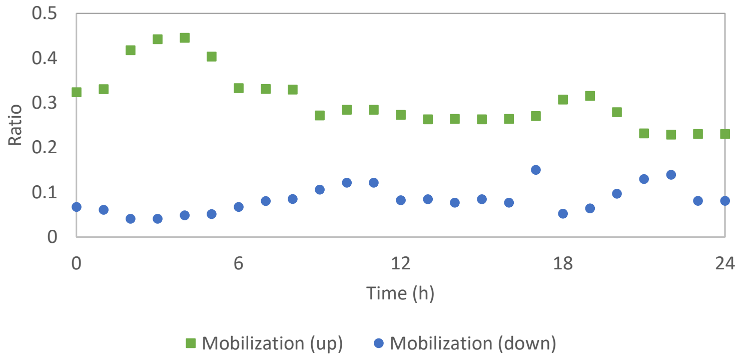

FIGURE 8 - DAY-AHEAD SECONDARY RESERVE ACTIVATION RATIOS

The real-time electricity energy and upward and downward secondary reserve activation prices are presented in Figure 9. The real-time electricity imbalance prices are presented Figure 10. The real-time activation ratios are presented in Figure 11. The gas imbalance prices was defined as 27.5 €/MWh.

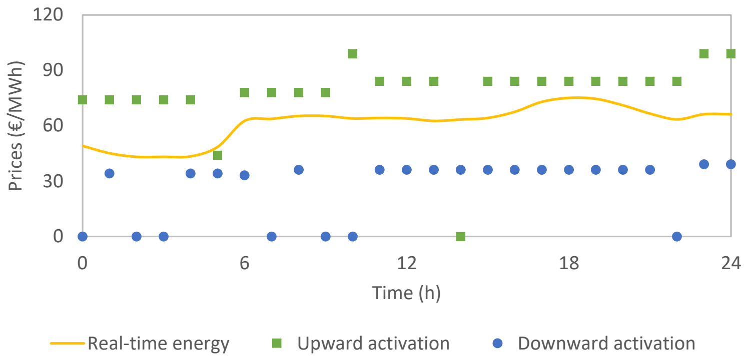

FIGURE 9 - REAL-TIME ELECTRICITY ENERGY AND SECONDARY RESERVE PRICES

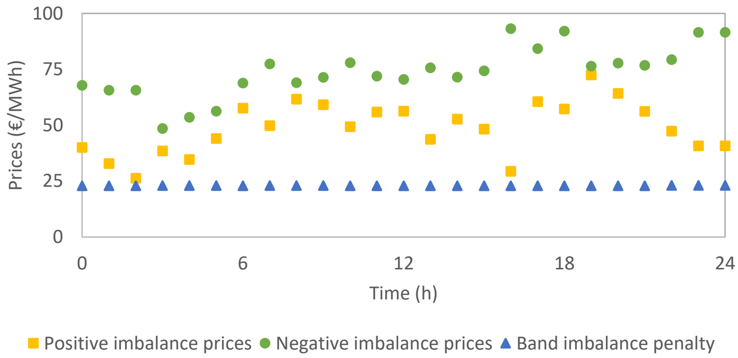

FIGURE 10 - REAL-TIME ELECTRICITY IMBALANCE PRICES

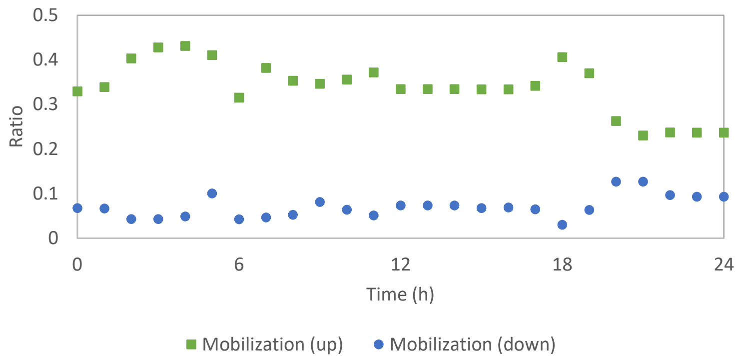

FIGURE 11 - REAL-TIME SECONDARY RESERVE ACTIVATION RATIOS

Figure 12 presents the solar profile and outside temperature day-ahead and real-time forecasts [14].

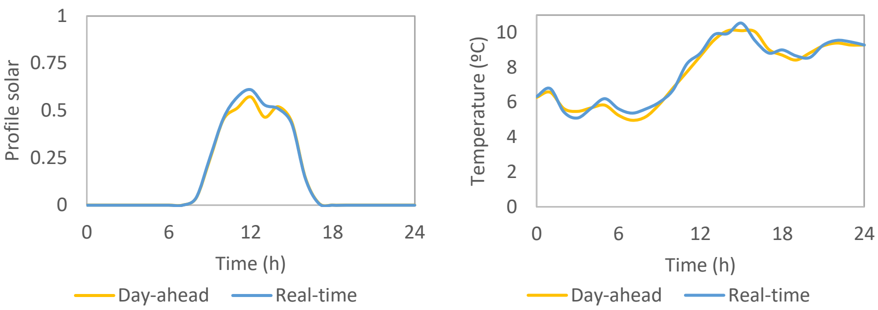

FIGURE 12 - DAY-AHEAD AND REAL-TIME SOLAR PROFILE AND OUTSIDE TEMPERATURE FORECASTS

The test cases were run in an Intel® Core™ i5.8265U CPU @ at 1.6GHz with 8 GB RAM on a Windows 10 operating system.

7.2. ADMM

7.2.1. Day-ahead

In the day-ahead tool, the ADMM converged in 214 iterations. It is possible to observe its convergence in Figure 13.

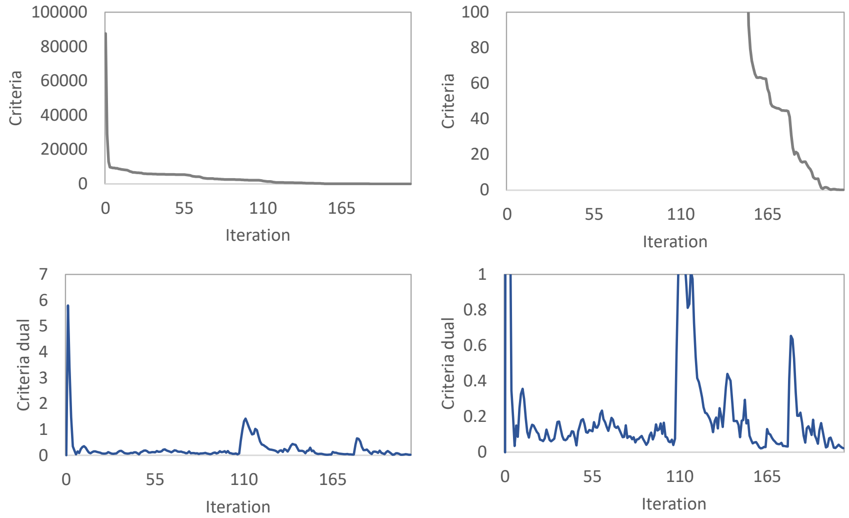

FIGURE 13 - CRITERIA AND CRITERIA DUAL OF THE DAY-AHEAD TEST

The optimization times of the optimizers *CPLEX* and *IPOPT* in each stage of the ADMM are presented in table Table 13. It is possible to observe that the step that consumes more time is the heat flow. The total optimization time was higher than 4h.

TABLE 13 - TIMES OF THE OPTIMIZERS IN EACH STAGE

		Aggregator	Power flow	Gas flow	Heat flow
Pre-negotiation	Per hour (s)	-	-	-	1.48
	Per iteration (s)	0.13	-	-	35.54
	Total (s)	2.18	-	-	604.25
	Sum total (min)	10.11			
Negotiation	Per hour (s)	-	0.05	0.10	1.01
	Per iteration (s)	0.51	2.21	2.28	72.72
	Total (s)	109	470	486	15489
	Sum total (min)	275.9			
Algorithm	Sum total (h)	4.8			

7.2.2. Real-time

The number of iterations until convergence per hour of the real-time tool are presented in table Table 14. It is possible to observe that they range from a minimum of 6 iterations to 267 iterations.

TABLE 14 - NUMBER OF ITERATIONS OF THE REAL-TIME TOOL

Hour	0	1	2	3	4	5	6	7	8	9	10	11
Number iterations	17	250	259	45	7	16	52	7	5	3	5	8
Hour	12	13	14	15	16	17	18	19	20	21	22	23
Number iterations	5	11	14	50	40	41	45	45	44	266	267	53

The optimization times per hour were similar to the times from the day-ahead tool.

7.3. Outputs

7.3.1. Day-ahead

Figure 14 presents the energy bids of the aggregator obtained from the day-ahead tool. These are aggregated bids per hour and they include energy bids and upward and downward secondary reserve band bids. This is the final output from the ADMM algorithm and the aggregator submits these bids to the electricity markets.

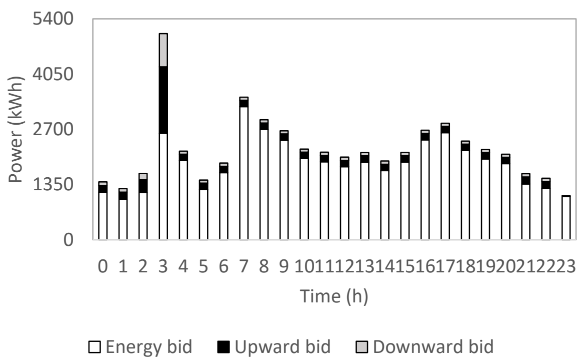

FIGURE 14 - DAY-AHEAD ELECTRICITY BIDS

Figure 15 presents the day-ahead gas bids submitted by the aggregator to the market.

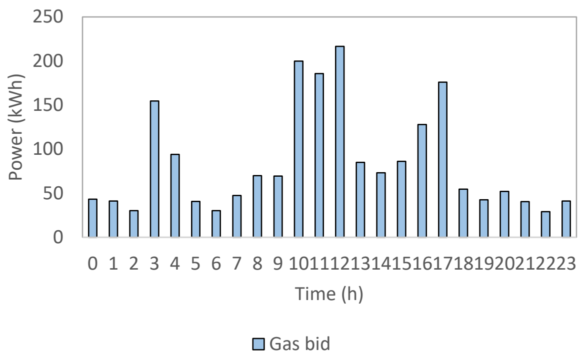

FIGURE 15 - DAY-AHEAD GAS BIDS

Figure 16 presents the energy bids and secondary reserve bands provided by the flexible resources. It is possible to observe that storage systems are the resources that provide flexibility more often.

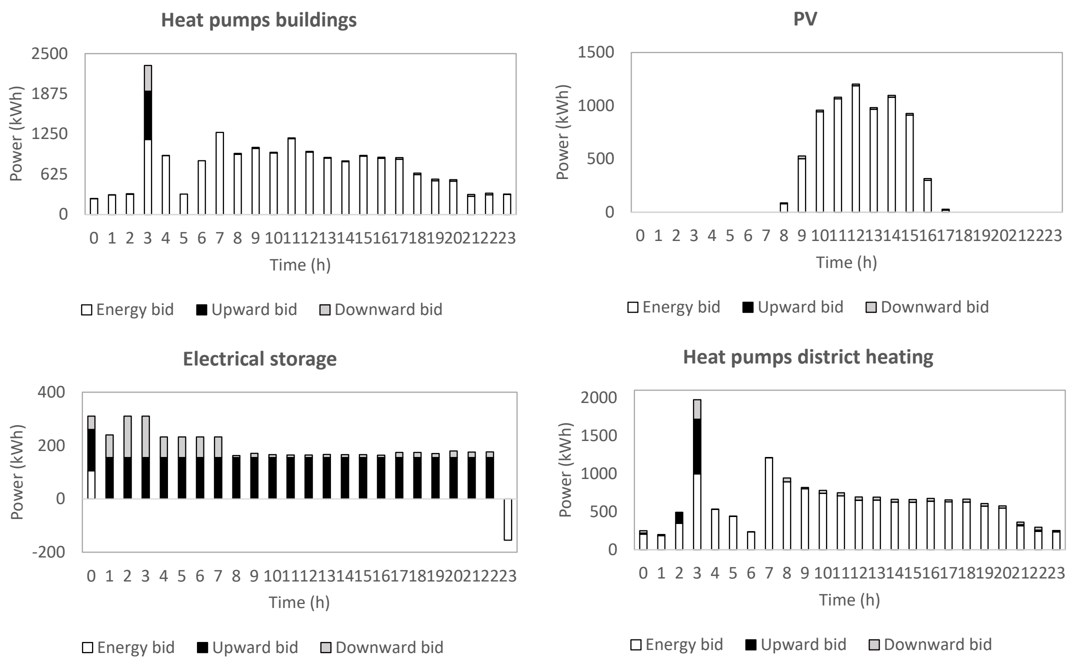

FIGURE 16 - DAY-AHEAD BIDS FROM FLEXIBLE RESOURCES

It is important to note that for simplification purposes these bids, as presented in this document, are cumulative of all electrical buses. The tool will provide these bids discriminated per electrical bus.

7.3.2. Real-time

In Figure 17 it is presented the results obtained from the level 1 of the real-time tool. The energy bids define the energy to be consumed/supplied at that hour and the upward and downward bids define the secondary reserve bands that the AGC can actually use in the next hour. These bids are different from the bids calculated from the day-ahead tool due to the new forecasted inputs, like a new solar profile, outside temperature or energy loads.

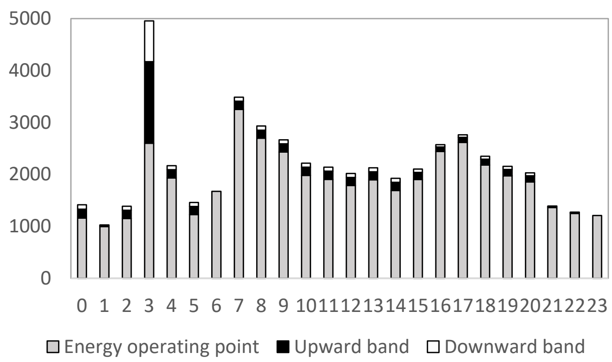

FIGURE 17 - REAL-TIME ENERGY AND SECONDARY RESERVE BAND

The energy imbalances in relation to the day-ahead bids are presented in Figure 18. It is possible to observe that at 6h there were only negative imbalances which can represent a surplus of demand or a shortage of generation.

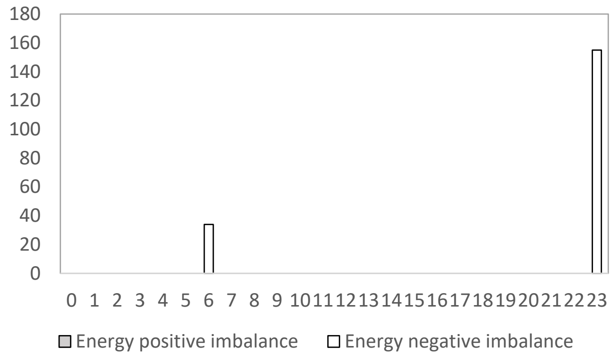

FIGURE 18 - REAL-TIME ENERGY IMBALANCES

Figure 19 presents the upward and downward secondary reserve band variation in relation to the day-ahead secondary reserve bands.

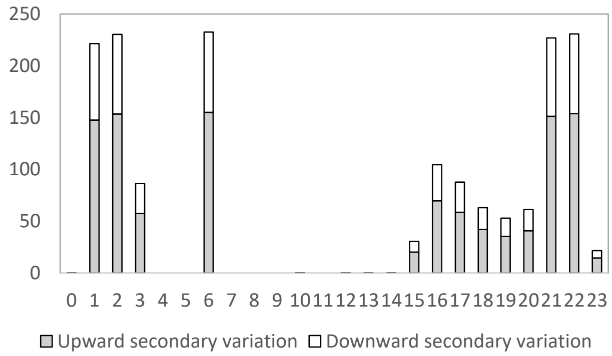

FIGURE 19 - REAL-TIME SECONDARY RESERVE BAND VARIATIONS

At level 2, the aggregator algorithm takes into account the AGC signal. This AGC signal is calculated considering the day-ahead energy and secondary reserve band bids presented in the market. If the real-time optimization of the aggregator defines the same bids and no imbalances occur, the AGC signal will be satisfied. This is possible to observe in Figure 20, where the power provided by the aggregator during that hour (black line) follows the AGC signal (red blocks), activating upward and downward band reserves.

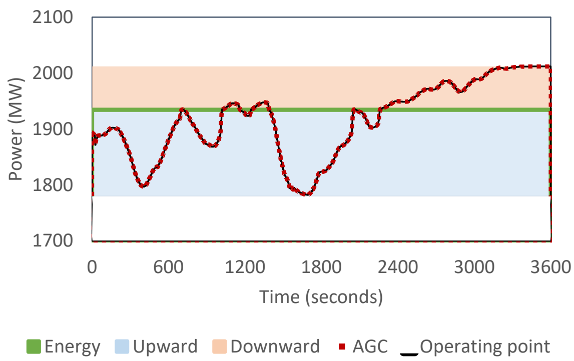

FIGURE 20 - OPERATING POINTS AND AGC SIGNAL, AT 4H

When imbalance occurs in the real-time optimization, the operating points of the aggregator will fail to follow the AGC signal, due to shortage of secondary reserve band, as it is possible to observe in Figure 21, for hour 2.

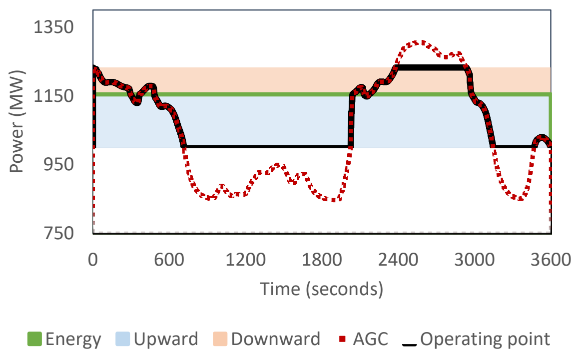

FIGURE 21 - OPERATING POINT AND AGC SIGNAL, AT 2H

The activated reserves are payed according to the operating point of the controller level.

7.4. Other results

This section includes some results related with the energy networks or the buildings to show the functioning of the tool in relation to these components.

Figure 22 presents the voltages obtained from the day-ahead tool for the electrical bus 14. It is possible to observe the difference between the upward and downward scenarios. As it would be expected, the upward scenarios present higher values of voltage as there is supposed to be more generation or less consumption. The same happens in Figure 23, where the voltages of all electrical buses at 9h are presented.

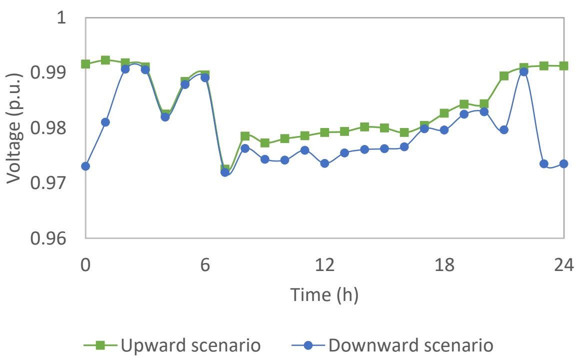

FIGURE 22 - VOLTAGES PER HOUR, AT BUS 14

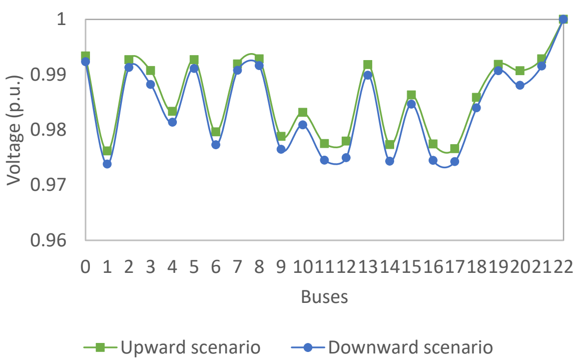

FIGURE 23 - VOLTAGES PER BUS, AT 9H

The temperatures in the district heating obtained from the day-ahead tool for node 14 during the day are presented in Figure 24. It is possible to observe different temperature profiles for the energy, upward and downward scenarios as they provide reserves in each scenario. Figure 25 shows the same information for 9h.

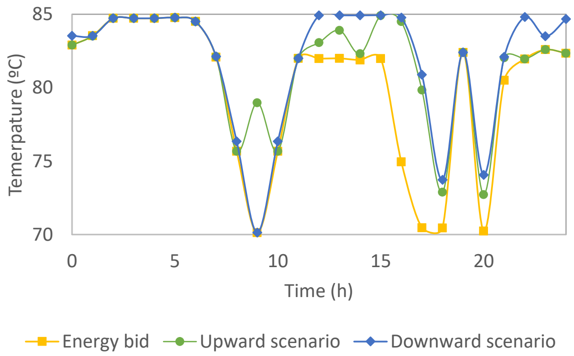

FIGURE 24 - DISTRIC HEATING TEMPERATURES IN EACH SCENARIO FOR NODE 14

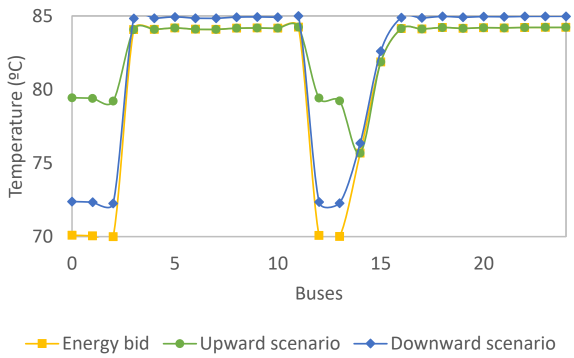

FIGURE 25 - DISTRICT HEATING TEMPERATURES FOR EACH SCENARIO AT 9H

In Figure 26 it is presented the electricity consumed or supplied in a building. It is possible to observe the consumption from the electrical load, the heat pump and the storage systems (positive values) as well as the electricity injected by the PV system and the storage system (negative values).

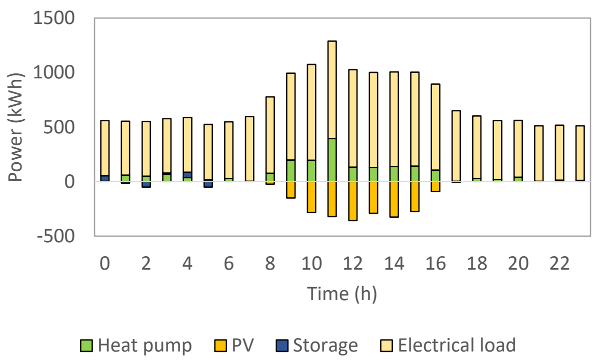

FIGURE 26 - ELECTRICITY CONSUMED/SUPPLIED IN A BUILDING

8. References

[1] J. Iria, F. Soares, and M. Matos, “Optimal bidding strategy for an aggregator of prosumers in energy and secondary reserve markets,” *Appl. Energy*, vol. 238, pp. 1361–1372, Mar. 2019.

[2] J. Iria and F. Soares, “Real-time provision of multiple electricity market products by an aggregator of prosumers,” *Appl. Energy*, vol. 255, p. 113792, Dec. 2019.

[3] J. Iria, P. Scott, and A. Attarha, “Network-constrained bidding optimization strategy for aggregators of prosumers,” *Energy*, vol. 207, p. 118266, Sep. 2020.

[4] A. Coelho, F. Soares, and J. Peças Lopes, “Flexibility Assessment of Multi-Energy Residential and Commercial Buildings,” *Energies*, vol. 13, no. 11, p. 2704, May 2020.

[5] A. Coelho, N. Neyestani, F. Soares, and J. P. Lopes, “Wind variability mitigation using multi-energy systems,” *Int. J. Electr. Power Energy Syst.*, vol. 118, p. 105755, Jun. 2020.

[6] Carlos M. Correa-Posada and P. Sánchez-Martín, “Gas Network Optimization: A comparison of Piecewise Linear Models,” *Lect. Notes Comput. Vis. Biomech.*, vol. 5, pp. 133–159, 2012.

[7] X. Liu, J. Wu, N. Jenkins, and A. Bagdanavicius, “Combined analysis of electricity and heat networks,” *Appl. Energy*, vol. 162, pp. 1238–1250, Jan. 2016.

[8] Y. Cao, W. Wei, L. Wu, S. Mei, M. Shahidehpour, and Z. Li, “Decentralized Operation of Interdependent Power Distribution Network and District Heating Network: A Market-Driven Approach,” *IEEE Trans. Smart Grid*, vol. 10, no. 5, pp. 5374–5385, Sep. 2018.

[9] E. A. M. Cesena, E. Loukarakis, N. Good, and P. Mancarella, “Integrated Electricity-Heat-Gas Systems: Techno-Economic Modeling, Optimization, and Application to Multienergy Districts,” *Proc. IEEE*, pp. 1–19, Jun. 2020.

[10] “Energy Information Administration (EIA)- Commercial Buildings Energy Consumption Survey (CBECS) Data.” [Online]. Available: https://www.eia.gov/consumption/commercial/data/2012/index.php?view=characteristics. [Accessed: 01-Dec-2020].

[11] ENTSO-E, “Transparency Platform.” [Online]. Available: https://transparency.entsoe.eu/dashboard/show. [Accessed: 24-Nov-2020].

[12] REN, “SIMEE - Mercado Diário e Intradiário.” [Online]. Available: https://www.mercado.ren.pt/PT/Electr/InfoMercado/InfOp/MercOmel/Paginas/default.aspx. [Accessed: 24-Nov-2020].

[13] M.-M. I. de Gás, “Preços diários da MIBGAS.” [Online]. Available: https://www.mibgas.es/pt/market-results. [Accessed: 24-Nov-2020].

[14] Meteogalicia, “Datos Históricos das redes de estacións.” [Online]. Available: https://www.meteogalicia.gal/web/inicio.action.

ANNEX I | INPUT DATA AND RESULTS FILES

This annex contains the information about the *Excel* files with input and output data as mentioned in Chapter 3.

Inputs

The inputs are organized in three files (Figure 27):

- "Input Data – Networks.xlsx" contains information about energy networks;
- "Input Data – Other.xlsx" contains information about weather forecasts, prices forecasts and ADMM settings;
- "Input Data – Resources.xlsx" contains information about resources.

Input Data - Networks.xlsx
Input Data - Other.xlsx
Input Data - Resources.xlsx

FIGURE 27 - INPUT FILES

Some examples of inputs present in each file are shown below.

Networks

The file "Input Data – Networks.xlsx" contains 11 pages where it is presented the electrical, gas and heat networks inputs. Table 15 presents the electrical branches inputs and Table 16 presents other necessary inputs to model the electrical network.

TABLE 15 - INPUTS OF PAGE "ELECTRICAL - BRANCH"

From	To	R (p.u.)	X (p.u.)
22	0	1.8762	2.5212
0	21	1.8762	2.5212
21	13	4.0639	5.4609
13	3	4.0771	5.4787
3	20	0.671	0.9017
0	18	5.1115	6.8685
18	10	2.0305	2.7285
10	12	4.1756	5.6109
12	11	2.7078	3.6386
11	16	0.6274	0.843
16	14	2.1157	2.843
0	15	5.6184	7.5497
15	4	2.4066	3.2339
4	6	3.54009	4.758
6	9	1.3649	1.8341
9	17	4.6369	6.2309
17	1	4.1682	5.6011
0	8	2.0804	2.7956
8	2	2.3038	3.0957

2	5	2.5241	3.3918
0	7	4.6178	6.2052
7	19	1.0629	1.4282
8	2	2.3038	3.0957
2	5	2.5241	3.3918
0	7	4.6178	6.2052
7	19	1.0629	1.4282

TABLE 16 - INPUTS OF PAGE "ELECTRICAL - OTHER"

Reference bus number	22
Reference bus voltage	1
System base (MVA)	1000
Maximum voltage (p.u.)	1.1
Minimum voltage (p.u.)	0.9
Maximum current (A)	500

Other

The file "Input Data – Other.xlsx" contains 3 pages where it is presented weather forecasts, price forecasts and ADMM settings. Table 17 presents the solar profile and outside temperature forecasts for 24h. Table 18 presents the ADMM settings.

TABLE 17 - INPUTS OF PAGE "WEATHER FORECASTS"

	Solar Profile	Outside temperature
1	0	6
2	0	7
3	0	6
4	0	5
5	0	6
6	0	6
7	0	5
8	0	5
9	0.038	5
10	0.242	6
11	0.454	7
12	0.513	8
13	0.572	9
14	0.465	11
15	0.521	10
16	0.439	10
17	0.144	10
18	0.009	9
19	0	9
20	0	8
21	0	9

22	0	9
23	0	9
24	0	9

TABLE 18 - INPUTS OF PAGE "ADMM"

Initial ro	0.0001
Stoping criteria	0.05

Resources

The file "Input Data – Resources.xlsx" contains 6 pages where it is presented electrical, gas and heat inflexible loads, type of resources and thermal models of loads/buildings/resources and the maximum and minimum temperature allowed in each thermal model. Table 19 presents the inflexible electrical load of 5 buildings for 24 hours. Table 20 presents the characteristics defined for 5 loads/buildings/resources.

TABLE 19 - INPUTS OF PAGE "ELECTRICAL LOAD"

Load/Building/Resource	1	2	3	4	5
1	63	45	5	17	0
2	62	43	6	18	0
3	58	42	5	18	0
4	61	41	6	22	0
5	58	41	6	21	0
6	60	41	6	21	0
7	61	40	6	18	0
8	80	50	11	21	0
9	95	50	23	38	0
10	115	64	25	38	0
11	129	68	24	42	0
12	129	66	25	41	0
13	130	66	27	38	0
14	136	66	23	39	0
15	131	62	21	44	0
16	127	65	21	45	0
17	124	68	17	40	0
18	108	68	13	28	0
19	95	68	8	20	0
20	85	69	7	20	0
21	78	68	6	18	0
22	63	53	7	17	0
23	61	50	6	13	0
24	60	48	5	17	0

TABLE 20 - INPUTS OF PAGE "LOADS, BUILDINGS, RESOURCES"

	Load/Building/Resource	1	2	3	4	5
Electrical heater	Installed (0-no,1-yes)	0	0	0	1	1
	Max power (kW)	0	0	0	1000	1000
	Efficiency/COP	0	0	0	3.45	3.45
Gas heater	Installed (0-no,1-yes)	0	0	0	0	0
	Max power (kW)	0	0	0	0	0
	Efficiency/COP	0	0	0	0	0
PV	Installed (0-no,1-yes)	0	0	0	1	0
	Max power (kW)	0	0	0	750	0
Storage	Installed (0-no,1-yes)	0	0	0	1	0
	Max power (kW)	0	0	0	100	0
	Max SOC (kWh)	0	0	0	250	0
	Min SOC (kWh)	0	0	0	15	0
	Initial SOC (kWh)	0	0	0	100	0
	Efficiency	0	0	0	0.9	0
District heating	Installed (0-no,1-yes)	1	1	1	0	0
	Max power (kW)	750	750	750	0	0
Gas	Load (0-no,1-yes)	1	0	1	1	0
Thermal model building	R (ºC/kWh)	0	0.081	0	0	0
	C (kWh/ºC)	0	437.7	0	0	0
	Initial temperature (ºC)	0	20	0	0	0

Outputs

The outputs of the day-ahead tool are organized in one file called “Bids_aggregator.xls” (Figure 28). The outputs of the real-time tool are organized in one file called “Bids_aggregator_RT.xls” (Figure 29).

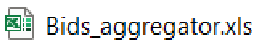

FIGURE 28 - OUTPUT FILE OF THE DAY-AHEAD TOOL

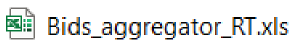

FIGURE 29 - OUTPUT FILE OF THE REAL-TIME TOOL

These files contain 4 pages where it is presented the electricity energy, upward and downward bids and the gas bids. Table 21 presents the electricity day-ahead energy bids obtained for 6 buses for 24h. Table 22 presents the day-ahead upward secondary band obtained for 6 buses for 24h.

TABLE 21 - OUTPUTS OF THE PAGE "ELECTRICITY ENERGY BID"

	0	1	2	3	4	5
0	0	35	0	17	18	188
1	0	32	0	8	16	156
2	0	35	0	17	18	159
3	0	31	696	17	16	179
4	0	35	0	20	17	167

5	0	30	0	19	15	172
6	0	41	0	47	21	198
7	0	55	0	39	28	204
8	0	88	0	124	44	274
9	0	87	0	134	44	150
10	0	117	0	81	58	-47
11	0	129	39	123	64	-47
12	0	174	36	130	87	-83
13	0	165	29	100	82	-34
14	0	154	32	73	77	-102
15	0	164	227	121	82	12
16	0	136	0	136	68	239
17	0	125	0	133	62	325
18	0	84	0	74	42	261
19	0	76	0	17	38	193
20	0	65	0	15	32	180
21	0	54	36	10	27	172
22	0	40	36	23	20	184
23	0	40	36	14	20	73

TABLE 22 - OUTPUTS OF THE PAGE "UPWARD SECONDARY BAND"

	0	1	2	3	4	5
0	0	0	4.1E-06	0	0	100
1	0	0	8.89E-06	0	0	100
2	0	0	0.000379	0	0	100
3	0	0	259.892	0	0	100
4	0	0	0.001103	0	0	100
5	0	0	9.96E-06	0	0	100
6	0	0	1.24E-06	0	0	100
7	0	0	1.04E-06	0	0	100
8	0	0	7.83E-07	0	0	100
9	0	0	5.51E-07	0	0	100
10	0	0	5.91E-07	0	0	100
11	0	0	6.52E-07	0	0	100
12	0	0	7.97E-07	0	0	100
13	0	0	7.76E-07	0	0	100
14	0	0	6.51E-07	0	0	100
15	0	0	5.54E-07	0	0	100
16	0	0	5.44E-07	0	0	100
17	0	0	4.86E-07	0	0	100
18	0	0	5.87E-07	0	0	100
19	0	0	5.89E-07	0	0	100
20	0	0	5.26E-07	0	0	100
21	0	0	6.36E-07	0	0	100
22	0	0	7.87E-07	0	0	100
23	0	0	1.6E-06	0	0	3.15E-06